

Anonymous Referee #1

General comments:

This manuscript presents the results of halocarbon measurement during a cruise campaign during the equatorial Atlantic Cold Tongue season. The importance of biological production in the surface water was confirmed and the production in the surface mixed layer was also suggested. In this study, the diapycnal fluxes and sea-air-exchange fluxes were investigated for the four halocarbons. Generally, the results and discussion are based on a well organized field campaign with quite high quality data and the manuscript is thoroughly prepared. I would like to recommend it to be published in Biogeosciences.

We thank anonymous referee #1 for the helpful input and suggestions. We refer to the specific comments in the following sections. Changes in the manuscript according to Anonymous Referee #1 are highlighted in red, while changes according to Anonymous Referee #2 are marked blue. Additional changes will be flagged in green.

Specific comments:

C5021

1. Page 5571, L14-26: In this part, the authors showed the correlations between halocarbons and other environmental/meteorological parameters and to give their suggestions. However, I found some of the correlations are too weak to support their points e.g. the correlation coefficient between CH₂I₂ and global radiation was only -0.25 and it seemed not solid enough.

We agree that the stated correlations are rather weak due to the interaction of sink and production processes. The anticorrelation of CH₂I₂ with global radiation for example is weakened by its daylight production, which leads to a less significant correlation as could be expected considering its very short lifetime (see section 5.3.3). However, as these weak correlations are significant, we think that it is worth mentioning these influence factors. We reworded several sentences and clarified in the corresponding sections that drawing conclusions from these correlations are subject to great uncertainty. We added some phrases in the discussion sections 5.1.1 and 5.1.2 to tone our statements based on the weaker correlations down.

For example:

Section 5.1.1:

“Although the correlation analysis of halocarbons with phytoplankton groups cannot directly resolve production and loss processes by algal activity, it is still an indicator for possible involvement of these species in halocarbon production.”

1 Section 5.1.2:

2 “The very low sea surface concentrations of CH_2I_2 with lowest concentrations during the day can be
3 explained by its fast photolysis (few minutes lifetime in surface sea water) (Jones and Carpenter,
4 2005; Martino et al., 2005).”

5

6 **2. Page 5576, L2-7: I do not understand why the strong negative correlations of**
7 **Prochlorococcus HL with $CHBr_3$ and CH_2Br_2 pointed to the association with warmer**
8 **oligotrophic water.**

9

10 We wanted to state that it’s more the other way round: the association of *Prochlorococcus* with warm
11 water leads to the strong non-causal negative correlation, since bromocarbons are associated with cold
12 water. The occurrence of *Prochlorococcus* in warm water can be observed via the correlation with
13 SST ($r_s = 0.44$, Table 2). This is not surprising since *Prochlorococcus* is one of the most abundant
14 phytoplankton groups in the tropical and subtropical ocean, and occurs in warmer water that is less
15 rich in nutrients (Johnson et al., 2006). On the other hand, bromocarbons correlated negatively with
16 SST, showing that these compounds were rather connected with cold water and species within the cold
17 water. *Prochlorococcus* were also most abundant north of the equator (see positive and significant
18 correlation with latitude of $r_s = 0.49$) where waters were warmer than in the southern transects of the
19 cruise. We modified this section in 5.1.1 as follows:

20

21 “These significant negative correlations can be explained by the large abundance of *Prochlorococcus*
22 in warm water, while bromocarbons on the other hand are more correlated with the cooler water of
23 the EUC, which is richer in nutrient and chrysophytes, haptophytes and dinoflagellates.”

24

25 **3. In the section 5.2, the distribution of halocarbon in the water column was not always**
26 **similar in the different locations. e.g. highest CH_2I_2 concentrations were measured in**
27 **the sea water layer of 0-30 m in CTD stations #4 and #6. As suggested by the authors, it**
28 **could be affected not only by the production but also but the sink process. I am curious**
29 **on how important the photolysis may be, especially for the shorter-lived CH_2I_2 . The**
30 **different local time for collection may lead to the different temperature, radiation etc.,**
31 **which seems not mentioned in the manuscript. More CH_2I_2 during night time should be**
32 **expected.**

33

34 We agree with the reviewer that the distribution of halocarbons within the water column may strongly
35 depend on the time of day. Photolysis is potentially the most important sink for CH_2I_2 in the surface
36 ocean, while the time scales for the other three mentioned compounds are much longer. For the
37 calculations of photolytical destruction in section 5.3, the diel cycle of radiation was of course

1 considered. We plotted the global radiation in Fig. 2c) as indicator for the time of day at which CTD
2 stations were performed (see also numbering of the CTD in the figure). While CTD station 4 was
3 carried out during noon, station 6 was indeed executed during night time. We checked the local time
4 for all of the other stations as well, and found no relationship between time of the day and the location
5 of the maximum in the CTD profiles, neither for bromocarbons nor for iodocarbons. The regional
6 variations in production seem to be much larger than the diel variability. We added a sentence
7 covering this aspect, since we consider this interesting information. We added to the end of section
8 5.2.:

9
10 *“Surprisingly, the time of day, influencing sink and production processes, seemed to play a minor role*
11 *for the shape of the profiles for all four compounds (see the location of the CTD stations in Fig. 2).”*
12

13 References:

14 Johnson, Z. I., Zinser, E. R., Coe, A., McNulty, N. P., Woodward, E. M. S., and Chisholm, S. W.:
15 Niche partitioning among prochlorococcus ecotypes along ocean-scale environmental gradients,
16 Science, 311, 1737-1740, 10.1126/science.1118052, 2006.

Anonymous Referee #2

This manuscript details the correlations between selected halocarbon concentrations (bromoform, dibromomethane, methyl iodide and diiodomethane) and the prevalence of certain plankton species in the equatorial Atlantic Cold Tongue. The authors assess the rates of production of these halocarbons accounting for air-sea gas exchange and diapycnal mixing. Overall, it is a useful contribution to the science examining the oceanic sources of these compounds to the atmosphere, and it should be published with minor revisions.

I agree with the approaches taken however, I do think the authors are attributing too much causation to correlation. The correlations are clear, however the cause may not be direct production by the organisms. It may be more related to the types of organic matter released. Recent results have shown that abiotic production of the brominated VSLs may be significant (Liu et al, 2013 and Liu et al, 2015). The authors need to address the impact that this source may play within in their data.

We thank Anonymous Referee #2 for the very valuable input. We agree that especially the very recent findings of Liu et al. (2015) are helpful to interpret field data. Unfortunately, this paper was not yet published when we submitted our study. We incorporate the discussion regarding DOM as potential substrate into the discussion section 5.1. We added to section 5.1.1:

*“It has been suggested that CHBr_3 is not produced directly from phytoplankton, but rather from dissolved organic matter (DOM) present in sea water (Lin and Manley, 2012). This was more closely investigated in laboratory experiments by Liu et al. (2015), who suggested that the weak in-situ correlations of bromocarbons with Chl *a* are a result of this indirect production pathway. The correlation with certain phytoplankton groups may then be caused by the production of phytoplankton-specific DOM.”*

As we stated in the answer to Anonymous referee #1, we now clearer emphasize the uncertainties associated with correlations in our manuscript. Changes in the manuscript according to Anonymous Referee #1 are highlighted in red, while changes according to Anonymous Referee #2 are marked blue. Additional changes are flagged in green.

1 **Specific Items:**

2 **Page 5570, first paragraph. There is additional Atlantic data not reported here. See Liu**
3 **et al, 2013.**

4
5 Thank you for making us aware of these data. It is correct, Liu et al. (2013) is missing here.
6 We will add the comparison with their data for the tropical region of the Atlantic around the
7 equator in section 4.1.1. We added:

8
9 *“Values of up to 10 pmol L⁻¹ (CHBr₃) and 3 pmol L⁻¹ (CH₂Br₂) near the equator were*
10 *reported by Liu et al. (2013b). The latter study covers the region during October and*
11 *November, indicating that the equatorial Atlantic seems to be a larger source for*
12 *bromocarbons during the intense cooling in the summer months.”*

13
14 **Page 5572, line 6 - what is meant by the parenthetical expression (in both cases profile**
15 **4)?**

16
17 To make the point clearer, we deleted the sentence and wrote instead:

18
19 *“The highest deep maximum concentrations of both CHBr₃ (up to 19.2 pmol L⁻¹) and CH₂Br₂*
20 *(up to 10.6 pmol L⁻¹) were observed in profile 4.”*

21
22 **Page 5582, line 8 - 'Only' should not be capitalized.**

23
24 We corrected this.

25
26 References added:

27 Lin, C. Y., and Manley, S. L.: Bromoform production from seawater treated with
28 bromoperoxidase, *Limnol. Oceanogr.*, 57, 1857-1866, 10.4319/1o.2012.57.06.1857, 2012.

29 Liu, Y. N., Yvon-Lewis, S. A., Thornton, D. C. O., Butler, J. H., Bianchi, T. S., Cambell, L.,
30 Hu, L., and Smith, R. W.: Spatial and temporal distributions of bromoform and
31 dibromomethane in the atlantic ocean and their relationship with photosynthetic biomass, *J.*
32 *Geophys. Res.-Oceans*, 118, 3950-3965, 10.1002/jgrc.20299, 2013b.

33 Liu, Y. N., Thornton, D. C. O., Bianchi, T. S., Arnold, W. A., Shields, M. R., Chen, J., and
34 Yvon-Lewis, S. A.: Dissolved organic matter composition driven the marine production of
35 brominated very short-lived substances, *Environ. Sci. Technol.*, 49, 3366-3374,
36 10.1021/es505464k, 2015.

37

1 **Halocarbon emissions and sources in the equatorial**
2 **Atlantic Cold Tongue**

3

4 **Helmke Hepach¹, Birgit Quack¹, Stefan Raimund¹, Tim Fischer¹, Elliot L. Atlas²,**
5 **and Astrid Bracher^{3,4}**

6 [1]GEOMAR Helmholtz-~~Zentrum~~ **Centre for für-Ozeanforschung Ocean Research** Kiel,
7 Germany

8 [2]Rosenstiel School of Marine and Atmospheric Science (RSMAS), University of Miami,
9 USA

10 [3]Helmholtz-University Young Investigators Group PHYTOOPTICS, Alfred-Wegener-
11 Institute (AWI) Helmholtz Center for Polar and Marine Research, Bremerhaven

12 [4]Institute of Environmental Physics, University of Bremen, Germany

13

14 Corresponding author: H. Hepach, GEOMAR Helmholtz-~~Zentrum~~ **Centre für for**
15 **Ozeanforschung Ocean Research** Kiel, Germany, Research Division 2: Marine
16 Biogeochemistry, Chemical Oceanography Düsternbrooker Weg 20, 24105 Kiel, Germany
17 (hhepach@geomar.de)

18

19

20

21

22

23

24

25

26

27

28

29

30

31

32

33

1 **Abstract**

2 Halocarbons from oceanic sources contribute to halogens in the troposphere, and can be
3 transported into the stratosphere where they take part in ozone depletion. This paper presents
4 distribution and sources in the equatorial Atlantic from June and July 2011 of the four
5 compounds bromoform (CHBr_3), dibromomethane (CH_2Br_2), methyl iodide (CH_3I) and
6 diiodomethane (CH_2I_2). Enhanced biological production during the Atlantic Cold Tongue
7 (ACT) season, indicated by phytoplankton pigment concentrations, led to elevated
8 concentrations of CHBr_3 of up to 44.7 pmol L^{-1} and up to 9.2 pmol L^{-1} for CH_2Br_2 in surface
9 water, which is comparable to other tropical upwelling systems. While both compounds
10 correlated very well with each other in the surface water, CH_2Br_2 was often more elevated in
11 greater depth than CHBr_3 , which showed maxima in the vicinity of the deep chlorophyll
12 maximum. The deeper maximum of CH_2Br_2 indicates an additional source in comparison to
13 CHBr_3 or a slower degradation of CH_2Br_2 . Concentrations of CH_3I of up to 12.8 pmol L^{-1} in
14 the surface water were measured. In contrary to expectations of a predominantly
15 photochemical source in the tropical ocean, its distribution was mostly in agreement with
16 biological parameters, indicating a biological source. CH_2I_2 was very low in the near surface
17 water with maximum concentrations of only 3.7 pmol L^{-1} , ~~and the observed anticorrelation~~
18 ~~with global radiation was likely due to its strong photolysis.~~ CH_2I_2 showed distinct
19 maxima in deeper waters similar to CH_2Br_2 . For the first time, diapycnal fluxes of the four
20 halocarbons from the upper thermocline into and out of the mixed layer were determined.
21 These fluxes were low in comparison to the halocarbon sea-to-air fluxes. **This indicates that**
22 **despite the observed maximum concentrations at depth, production in the surface mixed**
23 **layer is the main oceanic source for all four compounds and one of the main driving**
24 **factors of their emissions into the atmosphere in the ACT-region. The calculated**
25 **production rates of the compounds in the mixed layer are $34 \pm 65 \text{ pmol m}^{-3} \text{ h}^{-1}$ for**
26 **CHBr_3 , $10 \pm 12 \text{ pmol m}^{-3} \text{ h}^{-1}$ for CH_2Br_2 , $21 \pm 24 \text{ pmol m}^{-3} \text{ h}^{-1}$ for CH_3I and 384 ± 318**
27 **$\text{pmol m}^{-3} \text{ h}^{-1}$ for CH_2I_2 determined from 13 depth profiles.**

28

29 **1 Introduction**

30 Oceanic upwelling regions where cold nutrient rich water is brought to the surface are
31 connected to enhanced primary production and elevated halocarbon production, especially of
32 bromoform (CHBr_3) and dibromomethane (CH_2Br_2) (Quack et al., 2007a; Carpenter et al.,
33 2009; Raimund et al., 2011; Hepach et al., 2014). Photochemical formation (Moore and
34 Zafiriou, 1994; Richter and Wallace, 2004) with a possible involvement of organic precursors

1 is an important source for methyl iodide (CH_3I). An abiotic formation pathway for
2 halocarbons involving ozone has been found for diiodomethane (CH_2I_2) in the laboratory
3 (Martino et al., 2009). But, its production is generally suggested to be biotic, occurring likely
4 through different species of phytoplankton than are involved in the production of CHBr_3 and
5 CH_2Br_2 (Moore et al., 1996; Orlikowska and Schulz-Bull, 2009). Additionally, bacterial
6 involvement in the formation of halocarbons e.g. CH_3I and CH_2I_2 has been observed in the
7 field and the laboratory (Manley and Dastoor, 1988; Amachi et al., 2001; Fuse et al., 2003;
8 Amachi, 2008). Large uncertainties regarding the production of halocarbons in the ocean
9 remain. Depth profiles of the different compounds provide insight into the processes
10 participating in their cycling. Elevated concentrations of CHBr_3 and CH_2Br_2 at the bottom of
11 the mixed layer and below, often close to the chlorophyll *a* (Chl *a*) subsurface maximum, are
12 a common feature in the water column (Yamamoto et al., 2001; Quack et al., 2004; Liu et al.,
13 2013a), and are attributed to enhanced production by phytoplankton. While occasionally CH_3I
14 maxima close to the Chl *a* maximum were observed as well (Moore and Groszko, 1999;
15 Wang et al., 2009), Happell and Wallace (1996) ascribed surface maxima in several oceanic
16 regions including the equatorial Atlantic to a predominantly photochemical source. Rapid
17 photolysis and biogenic sources in the deep Chl *a* maximum are suggested to determine the
18 depth distribution of CH_2I_2 concentrations (Moore and Tokarczyk, 1993; Yamamoto et al.,
19 2001; Carpenter et al., 2007; Kurihara et al., 2010). The complex interactions between the
20 sources (biogenic and non-biogenic production), sinks (hydrolysis, photolysis, chlorine
21 substitution and air-sea gas exchange), advection, and turbulent mixing in and out of the
22 mixed layer (diapycnal fluxes), which determine the water concentrations of these
23 compounds, are still sparsely investigated.

24 Once they are produced in the ocean, halocarbons can be transported from the oceanic mixed
25 layer into the troposphere via air-sea gas transfer. CHBr_3 and CH_2Br_2 are the largest
26 contributors to atmospheric organic bromine from the ocean (Penkett et al., 1985; Schauffler
27 et al., 1998; Hossaini et al., 2012). Marine CH_3I is the most abundant organoiodine in the
28 troposphere, while the very short lived CH_2I_2 and CH_2ClI contribute potentially as much
29 organic iodine (Saiz-Lopez et al., 2012). Significant amounts of halocarbons and their
30 degradation products can be carried into the stratosphere (Solomon et al., 1994; Hossaini et
31 al., 2010; Aschmann et al., 2011), especially in the tropical regions where surface air can be
32 transported very rapidly into the tropical tropopause layer by tropical deep convection
33 (Tegtmeier et al., 2012; Tegtmeier et al., 2013). The short-lived brominated and iodinated

1 halocarbons produced in the equatorial region may hence play an important role for
2 stratospheric halogens.

3 This paper characterizes the distribution of CHBr_3 , CH_2Br_2 , CH_3I , and CH_2I_2 in the surface
4 water and the water column of the equatorial Atlantic Cold Tongue (ACT) for the first time.
5 The ACT is a known feature in the equatorial region, which is characterized by intensive
6 cooling of SSTs. This cooling is also associated with phytoplankton blooms (Grotsky et al.,
7 2008) as potential source for halocarbons. CHBr_3 , CH_2Br_2 , CH_3I and CH_2I_2 represent the most
8 important carriers of organic halogens into the troposphere, which have important
9 implications for atmospheric chemistry and are poorly characterized in the ACT region. We
10 therefore aim to provide more insight into the biological and physical processes contributing
11 to the mixed layer budget of halocarbons in the equatorial Atlantic. Sea-to-air fluxes and, for
12 the first time, diapycnal fluxes from the upper thermocline are calculated as sources and sinks
13 for the mixed layer. Phytoplankton groups (obtained from pigment concentrations) are
14 evaluated as potential sources of these four compounds. Additionally, surface water
15 halocarbons are correlated to meta data such as temperature, salinity and global radiation to
16 understand their distribution further. Finally, we estimate production rates for the mixed layer
17 of the ACT region.

18

19 **2 Methods**

20 Cruise MSM18/3 onboard the RV *Maria S. Merian* took place from June 21 to July 21 2011.
21 One goal of the campaign was the characterization of the Atlantic equatorial upwelling with
22 regard to halocarbon emissions and their sources. RV *Maria S. Merian* started in Mindelo
23 (Sao Vicente, Cape Verde) at 16.9° N and 25.0° W , and finished in Libreville (Gabon) at
24 0.4° N and 13.4° E with several transects across the equator. The ship entered the ACT
25 several times. Measurements of halocarbons and phytoplankton pigments were conducted in
26 surface water along the cruise track, and at 13 stations (Figure 1). Samples for dissolved
27 halocarbons from sea surface water were taken from a continuously working pump in the
28 ships moon pool at a depth of about 6.5 m every 3 h. Deep water samples were taken from up
29 to eight different depths per station between 10 and 700 m from 12 L Niskin bottles attached
30 to a 24-bottle-rosette with a CTD (Conductivity Temperature Depth). Halocarbon stations 1 –
31 4 were located at the first meridional transect across the ACT at 15° W , stations 5 – 7 at the
32 second transect at 10° W , 8 – 10 were located at the third section at around 5° W , and the last
33 three stations 11 – 13 were taken during the last section at 0° E (Figure 1). Water temperature
34 and salinity were recorded with a thermosalinograph. Air pressure and wind speed were

1 derived from sensors in 30 m height, averaged in 10 min intervals, **and wind speed was**
2 **corrected to 10 m**. Global radiation was measured onboard in 19.5 m height with sensors
3 (SMS-1 combined system from MesSen Nord, Germany) measuring downward incoming
4 global radiation (GS, shortwave) and infrared radiation (IR, long-wave).

5 **2.1 Sampling and analysis of halocarbons in seawater**

6 A purge and trap system attached to a gas chromatograph with mass spectrometric detection
7 (GC-MS) in single ion mode was used to analyze 50 mL water samples for dissolved
8 halocarbons. Volumetrically prepared standards in methanol were used for quantification.
9 Precision lay within 3 % for CHBr_3 , 6 % for CH_2Br_2 , 15 % for CH_3I and 20 % for CH_2I_2
10 determined from duplicates. For a detailed description see Hepach et al. (2014).

11 **2.2 Phytoplankton pigment analysis and continuous measurement of** 12 **chlorophyll a**

13 Water samples were filtered onto GF/F filters, shock-frozen in liquid nitrogen and stored
14 at -80°C . Pigments listed in Table 1 of Taylor et al. (2011) were analyzed using a HPLC
15 technique according to Barlow et al. (1997) as described in Taylor et al. (2011). **Surface**
16 **pigment data were already used in a study by Bracher et al. (2015). All pigment data are**
17 **already published and available from PANGAEA**
18 **(<http://doi.pangaea.de/10.1594/PANGAEA.848586>).** For interpretation of the pigment data,
19 CHEMTAX® (Mackey et al., 1996) was used, and initiated with the pigment ratio matrix
20 proposed by Veldhuis and Kraay (2004) for the subtropical Atlantic Ocean. The following
21 phytoplankton groups were evaluated: *diatoms*, *Synechococcus*-type, *Prochlorococcus* HL
22 (high light adapted) and *Prochlorococcus* LL (low light adapted), *dinoflagellates*,
23 *haptophytes*, *pelagophytes*, *cryptophytes* and *prasinophytes*.

24 10-min-averaged continuous surface maximum fluorescence measured by a microFlu-chl
25 fluorometer from TriOS located in the ships moon pool was used to derive continuous total
26 Chl *a* (TChl *a*) concentrations along the underway transect. This is based on the assumption
27 that active fluorescence *F* is correlated to the amount of available TChl *a* (Kolber and
28 Falkowski, 1993). The method to convert fluorescence to TChl *a* is described in detail in
29 Taylor et al. (2011). Mean conversion factors specific for each zone were determined for
30 collocated *F* and HPLC-TChl *a* (the sum of monovinyl Chl *a*, divinyl Chl *a* and
31 Chlorophyllide *a*; the latter is mainly formed as artefact of the former two during the
32 extraction process and therefore included in the calculation) measurements. A linear
33 regression of $r = 0.83$ ($p < 0.01$, $n = 89$) was observed between surface HPLC-derived TChl *a*
34 and *F*-derived TChl *a*, which indicates the robustness of the conversion of *F* to TChl *a*. The

1 high depth resolved chlorophyll profiles were derived from fluorescence values obtained from
2 a Dr. Haardt fluoremeter mounted to the CTD and calibrated with collocated HPLC-derived
3 TChl *a* concentrations at six depths of each profile according to Fujiki et al. (2011).

4 **2.3 Correlation analysis of halocarbons**

5 Different parameters were correlated to surface water halocarbons. Physical influences were
6 investigated with 10 min averages of sea surface temperature (SST), sea surface salinity
7 (SSS), global radiation and wind speed, and a relationship with location was explored using
8 latitude. Biological parameters used for correlations were TChl *a*, and the abundances of all
9 phytoplankton groups. Since most of the data sets were not normally distributed and common
10 transformations into normal distributions were not possible, the Spearman's rank correlation
11 coefficient r_s was applied. All correlations with $p < 0.05$ were regarded as significant.

12 Correlation analysis of the entire depth profile dataset using the Spearman's rank coefficient
13 did not allow for drawing specific conclusions due to the complexity of the data set. Hence,
14 the mixed influences on water column halocarbon concentrations were examined with
15 principal component analysis (PCA) using MATLAB®. PCA analyzes the collective variance
16 of a dataset including several variables. The PCA has the advantage to simplify a complex
17 data set and find similarities. Concentrations of all four halocarbons, all phytoplankton
18 groups, the TChl *a*, density, temperature, and salinity were included.

19 **2.4 Mixed layer depth**

20 Mixed layer depths z_{ML} were determined using the method introduced by Kara et al. (2000). It
21 proved to be closest to the visually determined z_{ML} from the temperature, salinity and density
22 profiles. The mixed layer of each CTD profile was calculated as the depth where the
23 temperature from the reference depth in the upper well-mixed temperature region was reduced
24 by a threshold value of 0.8 °C.

25 **2.5 Calculation of sea-to-air fluxes of halocarbons**

26 The air-sea gas exchange parameterization of Nightingale et al. (2000) was applied to
27 calculate sea-to-air fluxes F_{as} of halocarbons (equation 1). Schmidt number corrections as
28 reported by Quack and Wallace (2003) were applied to determine the compound specific
29 transfer coefficient k_w . The air-sea concentration gradient was computed from sea surface
30 water measurements and mean atmospheric mixing ratios c_{atm} of 2.50 ppt for CHBr₃, 1.20 ppt
31 for CH₂Br₂, and 0.50 ppt for CH₃I determined from 10 atmospheric data points during
32 MSM18/3, and atmospheric mixing ratios of 0.01 ppt for CH₂I₂ as reported by Jones et al.
33 (2010) for the tropical Atlantic. Henry's law constants H of Moore and co-workers (Moore et
34 al., 1995a; Moore et al., 1995b) were used to obtain the equilibrium concentrations c_{atm}/H .

$$F_{as} = k_w \cdot \left(c_w - \frac{c_{atm}}{H} \right) \quad (1)$$

2.6 Calculation of diapycnal fluxes of halocarbons

To estimate the halocarbon transport perpendicular to the stratification, equation 2 was used with F_{dia} as the diapycnal flux in $\text{mol m}^{-2} \text{s}^{-1}$, ρ as the seawater density in kg m^{-3} , Δc being the diapycnal gradient of the concentration in mol kg^{-1} , and K_{dia} as the diapycnal diffusion coefficient in $\text{m}^2 \text{s}^{-1}$.

$$F_{dia} = \rho \cdot K_{dia} \cdot \Delta c \quad (2)$$

In the equatorial near surface water, molecular and double diffusion are negligible compared to turbulent mixing. K_{dia} from turbulent mixing can be estimated from measurements of the velocity microstructure (turbulent motions on length scales of centimeters to meters). During MSM18/3, velocity microstructure profiling was performed immediately before or after taking halocarbon profiles, so that local and pointwise in time estimates of the diapycnal flux resulted from the combination of the two profiles via equation 2. The microstructure profiler (MSS) was a loosely tethered MSS90 equipped with airfoil shear probes, manufactured by Sea & Sun Technology. In order to calculate K_{dia} from velocity fluctuations measured by the MSS, first the average spectrum of vertical shear for a depth interval of typically 10 to 50 m was calculated and integrated to get an estimate of the average dissipation rate of turbulent kinetic energy (epsilon in W kg^{-1}). Equation 3, first proposed by Osborn (1980) allows to deduce K_{dia} , with γ a function of the mixing efficiency and N the buoyancy frequency for the chosen depth interval.

$$K_{dia} = \gamma \cdot \frac{\epsilon}{N^2} \quad (3)$$

γ was chosen to be 0.2 following Hummels et al. (2013) for the tropical Atlantic. A more detailed description of the method to derive K_{dia} and diapycnal fluxes below the mixed layer can be found in Schafstall et al. (2010), and Hummels et al. (2013), and Schlundt et al. (2014).

3 Physical and biological characteristics of the investigation area

3.1 Oceanographic description

The equatorial Atlantic is described by a complex current system. The surface is characterized by the westward South Equatorial Current (SEC), which spreads between 3° N and 15° S and reaches as deep as 100 m, but has shallow mixed layers close to the equator (Tomczak and Godfrey, 2005). The Equatorial Undercurrent (EUC) can be found below the SEC (Molinari, 1982), and is a narrow band between 2° N and 2° S flowing towards the east while reducing

1 speed. It carries mostly water with characteristics of deeper tropical surface water (TSW) and
2 of shallower central water. TSW around and north of the equator is characterized by high
3 temperatures and comparably low salinities due to enhanced precipitation (Tsuchiya et al.,
4 1992). While the core of the EUC in the west is at 100 m, its position in the east follows the
5 seasonal vertical migration of the thermocline (Stramma and Schott, 1999). In agreement with
6 this, the mixed layer depth was shallow and ranged only between surface and 49 m with a
7 mean of 28 m during MSM18/3. The mixed layer was also exposed to diurnal variability.
8 During daytime, it was shallower due to warmer air temperatures and more stratification. At
9 night, when the air temperature and SSTs cool, water mixes further down. The shallowest
10 mixed layers were found between 0° N and 3° S in agreement with the location of the EUC.
11 The Atlantic Cold Tongue (ACT) is a known feature in the equatorial region where SSTs
12 between 20° and 5° W can drop by 5 – 7 °C during May to September (Weingartner and
13 Weisberg, 1991). Many uncertainties remain with respect to the exact mechanisms that lead to
14 the development of the ACT. Jouanno et al. (2011) suggested that the strong increase of the
15 westward SEC associated with the ITCZ (Philander and Pacanowski, 1986), and the
16 maximum shear above the core of the underlying EUC lead to the low SSTs, confirmed later
17 by microstructure measurements (Hummels et al., 2013; [Schlundt et al., 2014](#)). Although the
18 shear is maximal at 0° E, maximum cooling appears at 10° W due to the stronger stratification
19 in the eastern basin of the equatorial Atlantic. SSTs during MSM18/3 of mean (range) 24.4
20 (22.1 – 29.0) °C and SSSs of 35.7 (34.5 – 36.3) were measured in the investigated region
21 (Table 1, Figure 2). Generally, high SSTs and low SSSs of less than 35.5 in the TSW were
22 observed north of the equator. Lower SSTs and higher SSSs were measured in the South
23 except for the 10° W section where these low SSTs and high SSSs were also found north of
24 the equator. Maximum SSTs around the equator of 28.5 °C were found at 3° N and 20° W,
25 while the lowest SSTs of 22.1 °C were located at 1° N and 10° W (Figure 1, Figure 2, Table
26 1).

27 **3.2 Biological description**

28 The cooling of SSTs in the ACT region is usually accompanied by a phytoplankton bloom.
29 Grodsky et al. (2008) found a seasonal peak of TChl *a* of 0.60 µg L⁻¹ in boreal summer. In
30 comparison, surface TChl *a* during MSM18/3 reached values as high as 1.20 µg L⁻¹ around
31 0.8° N and 0° E (Figure 2c). Very high TChl *a* concentrations above 1.00 µg L⁻¹ were also
32 measured from the continuous fluorescence sensor around 10° W, coincidentally with the
33 most intense cooling. The three hourly HPLC measurements of up to 0.99 µg L⁻¹ generally
34 also agree with the high TChl *a* maximum values measured with the fluorescence sensor (Fig.

1 2, Table 1). Additionally, nitrate and phosphate were significantly anticorrelated with SST
2 (not shown), hence the upwelled water of the EUC was connected to enhanced biological
3 production.
4 The most abundant phytoplankton group in the ACT were *chrysophytes* in both surface water
5 and depth profiles during MSM18/3 (Figure 2a). *Chrysophytes*, golden algae with flagellar
6 hairs, are thought to be mostly common in freshwater (Round, 1986). Nevertheless, they have
7 been previously shown to be also the most abundant phytoplankton group in several regions
8 of the Atlantic ocean, including the lower latitudes around the equator (Kirkham et al., 2011).
9 This group correlated significantly with SST ($r_s = -0.45$) and SSS ($r_s = 0.48$) (Table 2), it
10 hence seems to be associated with the upwelling water of the EUC. In the surface water,
11 *chlorophytes* and *Prochlorococcus* HL correlated positively with SST ($r_s = 0.13$, not
12 significant, and $r_s = 0.44$, significant) and negatively with SSS ($r_s = -0.15$, not significant, and
13 $r_s = -0.39$, significant). They were associated with warmer and less salty water masses than
14 *chrysophytes*, *dinoflagellates* and *haptophytes*. Thus, they were found predominantly north of
15 the equator. *Prochlorococcus* HL dominate among the species occurring from the surface
16 down to 50 m. *Prochlorococcus* LL, only observed in deeper layers (not shown here), were
17 the most abundant group from about 75 m downwards in the water column. These results are
18 in agreement with Johnson et al. (2006), where it was shown that *Prochlorococcus* dominate
19 in oligotrophic tropical waters, especially where nutrient concentrations are low at high
20 temperatures (between 15° S and 15° N of the Atlantic Ocean).

21

22 **4 Results**

23 **4.1 Surface water**

24 **4.1.1 CHBr₃ and CH₂Br₂**

25 Large regional variations were observed for the bromocarbons, especially for CHBr₃ in
26 surface water of the tropical Atlantic with a mean of 12.9 (1.8 – 44.7) pmol L⁻¹, and of 3.7
27 (0.9 – 9.2) pmol L⁻¹ for CH₂Br₂ (Figure 2, Table 1). Concentrations from the underway
28 measurements and from the shallowest profile depths (<10m) were included in the evaluation
29 of the surface water concentrations. The observed values are in agreement with data from the
30 tropical oligotrophic Atlantic north of 16° N and the Mauritanian upwelling ranging between
31 1.0 and 43.6 for CHBr₃ and 0.6 – 9.4 pmol L⁻¹ for CH₂Br₂ with the largest values close to the
32 coast and the upwelling (Quack et al., 2007a; Carpenter et al., 2009; Hepach et al., 2014).
33 Quack et al. (2004) observed lower CHBr₃ of 2.3 pmol L⁻¹ and CH₂Br₂ of 0.2 pmol L⁻¹ at
34 10° N through the tropical Atlantic in boreal fall and values of 12.8 and 5.3 pmol L⁻¹ for

1 CHBr₃ and CH₂Br₂ at the equator in agreement with our study. **Values of up to 10 pmol L⁻¹**
2 **(CHBr₃) and 3 pmol L⁻¹ (CH₂Br₂) near the equator were reported by Liu et al. (2013b).**
3 **The latter study covers the region during October and November, indicating that the**
4 **equatorial Atlantic seems to be a larger source for bromocarbons during the intense**
5 **cooling in the summer months.** Both compounds show the same pattern in surface water
6 throughout the MSM18/3 cruise with hot spots slightly south of the equator.
7 The very good correlation between CHBr₃ and CH₂Br₂ is in agreement with studies from
8 several regions, mostly attributed to related sources for both compounds from macro- and
9 microalgae (Nightingale et al., 1995; Moore et al., 1996; Schall et al., 1997; Laturus, 2001;
10 Quack et al., 2007b; Karlsson et al., 2008). Significant correlations to SST, SSS and TChl *a*
11 were found for CHBr₃ and CH₂Br₂, while very low insignificant correlations were observed
12 with the 10 min averaged global radiation values (Table 2). The **most-significant strongest**
13 correlations were found to *Prochlorococcus* HL with $r_s = -0.70$ for CHBr₃ and -0.57 for
14 CH₂Br₂, and to *chrysophytes* with $r_s = 0.43$, and $r_s = 0.41$, respectively.

15 **4.1.2 CH₃I and CH₂I₂**

16 The second highest mean sea surface water concentration was observed for CH₃I of 5.5 (1.5 –
17 12.8) pmol L⁻¹ (Figure 2, Table 1), which is in the range of earlier studies. These studies were widely
18 spread in the region from 20° S to 25° N between the coasts of South America and Africa with values
19 between 0 and 36.5 pmol L⁻¹ (Happell and Wallace, 1996; Schall et al., 1997; Richter and Wallace,
20 2004; Jones et al., 2010; Hepach et al., 2014). 7.1 to 16.4 pmol L⁻¹ were detected in the vicinity of our
21 investigated region (Richter and Wallace, 2004). CH₂I₂ was characterized by the lowest sea surface
22 water concentrations of 1.1 (0.3 – 3.7) pmol L⁻¹ **during MSM18/3**. Literature reports of CH₂I₂ in the
23 tropical Atlantic are very sparse: Schall et al. (1997) report on average three times higher values of 3.4
24 (2.1 – 6.8) pmol L⁻¹ in the tropical Atlantic, while Jones et al. (2010) measured a five times higher
25 mean of 5.8 (0.9 and 17.1) pmol L⁻¹ (reported in Ziska et al. (2013)) in the northern tropical Atlantic.
26 Similar to CHBr₃ and CH₂Br₂, sea surface CH₃I was significantly anticorrelated with SST ($r_s = -0.42$)
27 and not correlated with global radiation (Table 2). In contrast to the bromocarbons, correlations were
28 neither found to SSS, nor to latitude. Additionally, sea surface CH₃I correlated to biomass indicators
29 (TChl *a*: $r_s = 0.36$). The regional distribution of CH₃I often followed qualitatively that of *haptophytes*
30 ($r_s = 0.39$) with the most elevated concentrations south of the equator. Positive correlations were also
31 found to *dinoflagellates* ($r_s = 0.29$) and *chrysophytes* ($r_s = 0.26$). A weak, but significant
32 anticorrelation was observed to wind speed ($r_s = -0.22$). In contrast to the other three halocarbons,
33 CH₂I₂ was positively correlated with SST ($r_s = 0.33$), and elevated concentrations were observed
34 mostly north of the equator. A weak negative correlation of CH₂I₂ was found with global radiation
35 ($r_s = -0.25$), indicating higher sea surface CH₂I₂ during the night time and lower concentrations during
36 the day. CH₂I₂ correlated both with *chlorophytes* ($r_s = 0.32$) and *Prochlorococcus* HL ($r_s = 0.27$).

1 4.2 Water column

2 4.2.1 CHBr₃ and CH₂Br₂

3 CHBr₃ and CH₂Br₂ showed maxima at the surface, ~~below and at in~~ the ~~bottom~~ of the mixed
4 layer ~~and below it~~ (Figure 3, Table 3). ~~The highest deep maximum concentrations of both~~
5 ~~CHBr₃ (up to 19.2 pmol L⁻¹) and CH₂Br₂ (up to 10.6 pmol L⁻¹) were observed in profile~~
6 ~~4. Maximum deep concentrations of CHBr₃ reached values of up to 19.2 pmol L⁻¹, and~~
7 ~~up to 10.6 pmol L⁻¹ were observed in the deep maxima of CH₂Br₂ for bot(in both cases~~
8 ~~profile 4).~~ At stations where CHBr₃ was most elevated at the surface (profiles 2, 7, 12, 13),
9 much higher overall CHBr₃ concentrations of up to 35.0 pmol L⁻¹ were measured. CH₂Br₂
10 only reached maximum values of up to 6.6 pmol L⁻¹ in the surface (profiles 2, 7).

11 In contrast to surface water, CHBr₃ and CH₂Br₂ were distributed differently in the water
12 column with CH₂Br₂ being elevated 10 m below CHBr₃ in several profiles (Figure 3e). This
13 can also be seen in the T-S diagrams of these compounds (Figure 4a, b): while the most
14 elevated CHBr₃ was observed in the density layers between 1024 and 1025 kg m⁻³ (shallower
15 central water of the EUC), CH₂Br₂ was often also elevated in the denser, deeper layers below
16 30 m (Table 3). The maxima of both compounds were mostly in the vicinity of the TChl *a*
17 maximum. Results of the PCA (Figure 5) also show the dissimilarity of CHBr₃ and CH₂Br₂ at
18 depth: while the variance of CHBr₃ seems comparable to salinity and several phytoplankton
19 groups such as *chrysophytes*, CH₂Br₂ shows many similarities with the distribution of CH₂I₂
20 in the water column.

21 4.2.2 CH₃I and CH₂I₂

22 In agreement with CHBr₃ and CH₂Br₂, CH₃I was ~~both~~ elevated in the surface (three profiles
23 4, 6, 7) (Table 4, Figure 3b) with values of up to 12.8 pmol L⁻¹, and ~~also elevated~~ in the
24 deeper layers in and below the mixed layer (Figure 3f), reaching up to 8.5 pmol L⁻¹. Most
25 maxima of CH₃I were observed closer to the surface within the mixed layer (Figure 4d). The
26 PCA of CH₃I revealed that its variance was similar to the variance of *dinoflagellates* and
27 temperature (Figure 5).

28 CH₂I₂ was always depleted in the surface. Maxima of CH₂I₂ were found in different depths,
29 sometimes associated with the TChl *a* maximum (Figure 3f), and mostly below the mixed
30 layer (Figure 3j). The maxima in deeper depths appeared concurrently with the deeper CH₂Br₂
31 maxima (Figure 4), which is also expressed in the PCA (Figure 5). Values were generally
32 much higher in deeper depths with e.g. 13.8 pmol L⁻¹ between 60 and 100 m at profile 5. The
33 highest concentrations of the whole cruise of 16.0 pmol L⁻¹ (profile 1) were found between 30

1 and 60 m. Concentrations of only up to 12.0 pmol L⁻¹ were found between 0 and 30 m (profile
2 6) (Table 4).

3 **4.3 Fluxes**

4 **4.3.1 CHBr₃ and CH₂Br₂**

5 Sea-to-air fluxes of CHBr₃ and CH₂Br₂ of 644 (-146 – 4285) and 187 (-3 – 762) pmol m⁻² h⁻¹
6 during MSM18/3 were larger during the first two western NS-transects of the cruise which
7 were characterized by higher seawater concentrations, as well as higher wind speeds (Table 1,
8 Figure 6). Carpenter et al. (2009) and Hepach et al. (2014) reported -150 and 3504
9 pmol m⁻² h⁻¹ CHBr₃ fluxes as well as of 5 – 917 for CH₂Br₂ from the Cape Verde and
10 Mauritanian upwelling region. The lower fluxes in the equatorial region are a result of the
11 lower wind speeds measured during MSM18/3, ranging from 0.3 – 11.1 with a mean of 6.1
12 m s⁻¹, and the lower concentration gradients in comparison to Carpenter et al. (2009). Quack
13 et al. (2004) reported CHBr₃ fluxes from the equatorial Atlantic of 2700 (± 800) pmol m⁻² h⁻¹,
14 which compare well to this study.

15 Diapycnal fluxes are the fluxes of halocarbons that diffuse out or into the mixed layer from
16 below the thermocline. Maxima within the mixed layer will lead to fluxes towards the
17 thermocline, while maxima below the mixed layer will result in a flux of halocarbon-
18 molecules into the mixed layer. Diapycnal fluxes of halocarbons were generally low although
19 the EUC can lead to enhanced mixing. This is due to the comparably small concentration
20 gradients of the halocarbons. Diapycnal fluxes were 80 (CHBr₃) to 200 times (CH₂Br₂) lower
21 than sea-to-air fluxes (Table 5). They acted both as a source and a sink for halocarbons in the
22 mixed layer. At eight stations, CHBr₃ was diffusing into the mixed layer, providing on
23 average 5 (0 – 14) pmol m⁻² h⁻¹ from below to the mixed layer budget of CHBr₃. On the other
24 hand, on average 30 (2 – 125) pmol m⁻² h⁻¹ were diffusing out of the mixed layer, which is the
25 highest flux to the thermocline of all four halocarbons, as a result of its large concentration
26 gradients across the bottom of the mixed layer. Diapycnal fluxes of CH₂Br₂ were generally
27 lower than for CHBr₃ due to its lower concentration gradients. Its fluxes into the mixed layer
28 from eight profiles were on average 3 (0 – 8) pmol m⁻² h⁻¹, while the diapycnal flux reduced
29 the mixed layer budget of CH₂Br₂ by 2 (0 – 8) pmol m⁻² h⁻¹ at the remaining five stations.

30 **4.3.2 CH₃I and CH₂I₂**

31 CH₃I sea-to-air fluxes were on average 425 (34 – 1300) pmol m⁻² h⁻¹ during the cruise. During
32 the eastern NS-transects, fluxes were elevated at several locations mostly during daytime in
33 contrast to the bromocarbons, in accordance to a larger concentration gradient of CH₃I in that
34 region (Table 1, Figure 6). The fluxes are only half of the sea-to-air fluxes from the equatorial

1 Atlantic region reported by Richter and Wallace (2004) of $958 \pm 750 \text{ pmol m}^{-2} \text{ h}^{-1}$ and a fifth
2 of the fluxes reported from Jones et al. (2010) of on average $2154 \text{ pmol m}^{-2} \text{ h}^{-1}$ from the Cape
3 Verde and Mauritanian upwelling region. But, they were two times larger than the fluxes of
4 Hepach et al. (2014) of on average $246 \text{ pmol m}^{-2} \text{ h}^{-1}$. CH_2I_2 fluxes were generally larger in the
5 beginning of the cruise where higher wind speeds and higher surface water concentrations
6 existed. Only few studies have published sea-to-air fluxes of CH_2I_2 from the tropical ocean.
7 CH_2I_2 emissions calculated for MSM18/3 are with only $82 (3 - 382) \text{ pmol m}^{-2} \text{ h}^{-1}$ very low in
8 comparison to mean fluxes reported by Jones et al. (2010) of on average $541 -$
9 $688 \text{ pmol m}^{-2} \text{ h}^{-1}$, which are the result of higher oceanic CH_2I_2 (Jones et al., 2010).
10 Similar to the bromocarbons, diapycnal fluxes of CH_3I and CH_2I_2 were generally lower (117
11 and 7 times, respectively) than sea-to-air fluxes (Table 5). Due to the larger CH_3I
12 concentrations in the mixed layer compared to the upper thermocline, diapycnal fluxes of $5 (1$
13 $- 13) \text{ pmol m}^{-2} \text{ h}^{-1}$ were mostly acting as a sink for the mixed layer budget. Only at three
14 stations, $2 (1 - 5) \text{ pmol m}^{-2} \text{ h}^{-1}$ were transported into the mixed layer. Diapycnal fluxes of
15 CH_2I_2 acted mostly as source for the mixed layer, providing on average $12 (0 -$
16 $39) \text{ pmol m}^{-2} \text{ h}^{-1}$ due to its much higher concentrations in the water below. This represents the
17 highest halocarbon flux of the four compounds into the mixed layer. The diapycnal flux of
18 CH_2I_2 of $2 (0 - 4) \text{ pmol m}^{-2} \text{ h}^{-1}$ out of the mixed layer was only observed at three stations.

19

20 **5 Discussion**

21 **5.1 Surface water distribution**

22 **5.1.1 CHBr_3 and CH_2Br_2**

23 The equatorial Atlantic is a source of CHBr_3 and CH_2Br_2 to the atmosphere during the ACT
24 season, and the correlations of their water concentrations to biogenic parameters indicate
25 biological formation. CHBr_3 and CH_2Br_2 correlated significantly, but weakly with TChl *a*,
26 which is not an unusual feature (Abrahamsson et al., 2004a; Carpenter et al., 2009; Liu et al.,
27 2011; Hepach et al., 2014). **It has been suggested that CHBr_3 is not produced directly**
28 **from phytoplankton, but rather from dissolved organic matter (DOM) present in sea**
29 **water (Lin and Manley, 2012). This was more closely investigated in laboratory**
30 **experiments by Liu et al. (2015), who suggested that the weak in-situ correlations of**
31 **bromocarbons with Chl *a* are a result of this indirect production pathway. The**
32 **correlation with certain phytoplankton groups may then be caused by the production of**
33 **phytoplankton-specific DOM.** The very negative correlations of bromocarbons with SST
34 and positive correlations with SSS indicate a relationship of bromocarbon abundance with
35 processes within the cold and nutrient-rich upwelled water of the EUC (section 3.2),

1 supported by the T-S diagrams (Figure 4). Weak, but significant negative correlations with
2 latitude ($r_s = -0.38$ for CHBr_3 and $r_s = -0.18$ for CH_2Br_2) and maximum values of the
3 bromocarbons between 2 and 3° S, where EUC water reaches the surface, underline this
4 hypothesis. Although the correlation analysis of halocarbons with phytoplankton groups
5 cannot directly resolve production and loss processes by algal activity, it is still an indicator
6 **for potential sources for possible involvement of these species in halocarbon production.**
7 Bromocarbon production might exceed loss processes, which leads to the observed statistical
8 link of CHBr_3 and CH_2Br_2 to *chrysophytes*. *Chrysophytes* are to our knowledge not yet among
9 observed halocarbon producers in incubation and field studies. The strong negative
10 correlations of *Prochlorococcus* HL with CHBr_3 and CH_2Br_2 have been observed previously
11 (Hepach et al., 2014). **These significant negative correlations can be explained by the**
12 **large abundance of *Prochlorococcus* in warm water while bromocarbons on the other**
13 **hand are more correlated with the cooler water of It indicates the production of**
14 **bromocarbons in the colder and more biologically active water masses of the EUC, which**
15 **is are rich in richer in nutrients and *chrysophytes*, *haptophytes* and *dinoflagellates* (in the**
16 **order of significance). while *Prochlorococcus* HL is more associated with warmer**
17 **oligotrophic water leading to a significant correlation.**

18 5.1.2 CH_3I and CH_2I_2

19 ~~The anticorrelation of~~ CH_3I concentrations and wind speed **were weakly anticorrelated**
20 during MSM18/3. ~~was reported previously (Richter (2004) interprets this as depletion of~~
21 **the surface concentrations, when air-sea fluxes exceed the production rate during high**
22 **wind speeds. Low wind speed leads to lower sea-to-air fluxes, and thus an accumulation**
23 **of the produced CH_3I in the sea surface. High wind speeds deplete the surface when air-**
24 **sea fluxes exceed the production rate.** There are two production mechanisms suggested for
25 CH_3I . Previous studies (Richter and Wallace, 2004; Jones et al., 2010) have attributed CH_3I in
26 the tropical ocean mainly to photochemical formation based on the observations of Moore and
27 Zafiriou (1994). In contrast to these studies, indications for biological formation of CH_3I were
28 found in the ACT region during our study. CH_3I showed a **weak** negative correlation with
29 SST, significant correlations with the biologically produced CHBr_3 and CH_2Br_2 (Table 2) and
30 with TChl *a* as biomass indicator, and no correlation to global radiation. These imply a
31 relationship with the biologically active upwelled water. Elevated concentrations of CH_3I
32 were found between 10° and 5° W during midday (see CH_3I in comparison to global radiation
33 in Figure 2), which could be a result of photochemical formation. Thus we suggest that
34 photochemistry and biological production likely both played a role during MSM18/3.

1 *Haptophytes* correlated most significantly of the phytoplankton groups with CH₃I and have
2 already been shown to produce CH₃I both in the laboratory (Itoh et al., 1997; Manley and de
3 la Cuesta, 1997; Scarratt and Moore, 1998; Smythe-Wright et al., 2010) and in the field
4 (Abrahamsson et al., 2004b). Correlations during MSM18/3 **additionally** indicate **a possible**
5 **involvement** of *dinoflagellates* and *chrysophytes* **in the production of methyl iodide as**
6 **additional source organisms** (Table 2). **The importance of oceanic CH₃I production by**
7 ***Prochlorococcus* is a matter of dispute. Brownell et al. (2010) report it to be a minor**
8 **source, in contrast to both Smythe-Wright et al. (2006) and Hughes et al. (2010, 2011).**
9 **No evidence of involvement of *Prochlorococcus* HL was found during MSM18/3. which**
10 **have often been discussed as important source for CH₃I in the open ocean (Smythe-**
11 **Wright et al., 2006; Brownell et al., 2010; Hughes et al., 2011), had any influence on**
12 **surface CH₃I concentrations during MSM18/3.**

13 The very low sea surface concentrations of CH₂I₂ with lowest concentrations during the day
14 **are a result of can be explained** by its fast photolysis (few minutes lifetime in surface sea
15 water) **and it explains the negative correlation with global radiation during MSM18/3**
16 (Jones and Carpenter, 2005; Martino et al., 2005). Although CH₂I₂ is generally assumed to be
17 of biogenic origin in the open ocean (Moore and Tokarczyk, 1993; Yamamoto et al., 2001;
18 Orlikowska and Schulz-Bull, 2009; Hopkins et al., 2013), great uncertainties remain as to
19 which species are involved in its production. During MSM18/3, indications were found for
20 different source species than of the other three compounds (*chlorophytes* and
21 *Prochlorococcus* HL).

22 **5.2 Water column distribution**

23 Halocarbon maxima in the TChl *a* maximum, attributed to their biological production, are
24 often observed from polar to tropical regions (Moore and Tokarczyk, 1993; Moore and
25 Groszko, 1999; Yamamoto et al., 2001; Quack et al., 2004; Carpenter et al., 2007; Hughes et
26 al., 2009). In contrast, **a**-photochemical formation of CH₃I **leads can lead** to surface maxima
27 (Happell and Wallace, 1996). During MSM18/3, maxima of halocarbons were not always
28 found in the TChl *a* maximum. This does not contradict their biological production, as the
29 location of the TChl *a* maximum is not necessarily the location of highest biomass or primary
30 production, but rather reflects the photoadaptation capability of the predominant phytoplankton
31 groups (Claustre and Marty, 1995). Unfortunately, neither biomass nor primary production
32 was measured during the cruise. Additionally, halocarbons could be produced by
33 phytoplankton groups that are not in the maximum of the biomass distribution in the water
34 column, and the location of the halocarbon maximum might be more determined from their

1 sink processes than from their production. **Surprisingly, the time of day, influencing sink**
2 **and production processes, seemed to play a minor role for the shape of the profiles for**
3 **all four compounds (see the location of the CTD stations in Fig. 2).**

4 **5.2.1 CHBr₃ and CH₂Br₂**

5 In contrast to their similar occurrence in the surface, CHBr₃ and CH₂Br₂ showed different
6 distributions in the water column (Figure 5). Strong indications for biological sources of
7 CHBr₃ exist in the PCA, and *chrysophytes* as potential source group are in agreement to the
8 surface water observations (Table 2, Figure 5). Maximum CH₂Br₂ concentrations were
9 occasionally found below the CHBr₃ maxima, which have already been observed in the
10 Mauritanian upwelling (Quack et al., 2007b). The deeper maxima may be either due to an
11 additional source of CH₂Br₂ such as the biologically mediated conversion of CHBr₃ (Hughes
12 et al., 2013) or to a faster degradation of CHBr₃ than of CH₂Br₂ at depth. Sinks for CHBr₃ and
13 CH₂Br₂ in tropical surface waters include very slow hydrolysis (hundreds to thousands of
14 years) (Mabey and Mill, 1978) and slow halogen substitution (5 years) (Geen, 1992).
15 Photolysis, which has been suggested to be faster for CHBr₃ (9 years with a mixed layer of
16 100 m for CHBr₃) than for CH₂Br₂ (Carpenter et al., 2009) would be of more significance in
17 the surface layer. A faster degradation of CHBr₃ in greater depths is also somewhat contrary
18 to the observed very fast bacterial degradation of CH₂Br₂ with a half-life of 2 days (Goodwin
19 et al., 1998). An additional source for CH₂Br₂ that involves CHBr₃ therefore seems more
20 plausible. At four of the 13 stations, indications for the additional source were found. There,
21 maximum CH₂Br₂ concentrations were found below CHBr₃, which could be the result of its
22 faster conversion to CH₂Br₂ than its production. CH₂Br₂ in denser water is also co-located
23 with *Prochlorococcus* LL, which might be involved in the CHBr₃-conversion.

24 **5.2.2 CH₃I and CH₂I₂**

25 CH₃I was usually elevated in the top 30 m of the water column apart from three profiles,
26 where maximum concentrations were found between 30 and 60 m. The surface maxima, as
27 seen in the T-S diagram (Figure 4), support the photochemical formation of CH₃I (Happell
28 and Wallace, 1996). Deeper maxima could also arise if the sea-to-air flux exceeds the
29 photochemical production. However, the low wind speed during the cruise (section 3), the
30 relationship with biological parameters, and the partly co-located maxima with the other three
31 biogenic halocarbons (Figure 3, Figure 5) also point to a direct production of CH₃I from
32 phytoplankton. These include *dinoflagellates* as indicated by the correlations and the PCA
33 (Figure 5).

34 CH₂I₂ was always depleted in the surface with respect to the underlying water column as a
35 result of its strong photolysis (Jones and Carpenter, 2005; Martino et al., 2006). It was

1 frequently elevated below the TChl *a* maximum and below the base of the mixed layer
2 (Figure 3) in contrast to previous studies (Moore and Tokarczyk, 1993; Yamamoto et al.,
3 2001). The similarity in its distribution to CH₂Br₂ (Figure 4, Figure 5) could indicate similar
4 production and sink processes at depth. Bacterial formation of CH₂I₂ (Fuse et al., 2003;
5 Amachi et al., 2005) in the upper thermocline could also be an additional source for this
6 compound. Alternatively, CH₂I₂ may not degrade as quickly as CHBr₃ and CH₃I in greater
7 depths, which would lead to its accumulation below the mixed layer.

8 **5.3 Factors contributing to halocarbon emissions from the mixed layer**

9 Halocarbon emissions into the atmosphere depend strongly on the mixed layer budget of these
10 compounds, which is determined by their sources and sinks. It is unclear, where the main
11 halocarbon production occurs. It has been suggested that it takes mainly place in the
12 subsurface TChl *a* maximum (Quack et al., 2004; Martino et al., 2006), whereas other model
13 studies assume production of e.g. CHBr₃ to be coupled to primary production in the whole
14 water column (Hense and Quack, 2009). Assuming production of halocarbons takes place
15 mainly in the TChl *a* maximum, which is often located below the mixed layer, diapycnal
16 fluxes from below the thermocline will be the most important source for mixed layer
17 halocarbons.

18 **5.3.1 Transport and loss processes in the mixed layer**

19 To evaluate the significance of halocarbon production below the mixed layer for emissions
20 into the atmosphere, production, loss and transport processes have to be considered. The
21 diapycnal fluxes of the four halocarbons were calculated from 13 halocarbon profiles and
22 parallel measurements of eddy diffusivity (section 4.3). The data are characterized by a low
23 depth resolution of the halocarbons within the water column and a short validity of the
24 diffusion coefficients, which make the diapycnal fluxes subject to some uncertainties. Given
25 that the depth profiles measured during MSM18/3 agree well to previous studies from the
26 tropical ocean (Yamamoto et al., 2001; Quack et al., 2004), a general idea of the significance
27 of diapycnal fluxes for the mixed layer budget of halocarbons can be obtained. The chemical
28 loss rates are estimated from published data which include hydrolysis, halogen substitution
29 and photolysis. The half-lives of CHBr₃ and CH₂Br₂ due to hydrolysis are hundreds to
30 thousands of years (Mabey and Mill, 1978), while for CH₃I, the half-life due to hydrolysis
31 ranges from 1600 days at 25 °C to 4000 days at 5 °C (Elliott and Rowland, 1995). The half-
32 life of CHBr₃ with respect to photolysis is 9 years assuming a mixed layer depth of 100 m
33 and is potentially slower for CH₂Br₂ (Carpenter and Liss, 2000), halogen-substitution is 5
34 years in warm waters (Geen, 1992). ~~The half-life of CHBr₃ with respect to photolysis is 9~~
35 ~~years assuming a mixed layer depth of 100 m, and potentially slower for CH₂Br₂~~

1 (~~Carpenter et al., 2009~~). Liu et al. (2011) calculated the half-life of CHBr_3 due to photolysis
 2 in a coastal mixed layer of 5 m to be only 82 days. ~~Since~~ Mixed layers during MSM18/3 were
 3 from ~~surface to down to~~ 49 m, photolysis of bromocarbons in the mixed layer will ~~also~~ lead
 4 to ~~shorter~~ half-lives of several months. Sea-to-air flux is the most significant sink for CHBr_3
 5 and CH_2Br_2 from the mixed layer. Mean half-lives of 8 days were calculated for both
 6 compounds during MSM18/3, based on the fluxes (section 4.3.1) and the mixed layer depths
 7 during the cruise (Table 3). We consider a very short time scale of 1 h for our budget
 8 calculations due to the validity of the diapycnal flux coefficients, while the general findings of
 9 our calculations are also valid for a longer time scale. As the sink from the mixed layer due to
 10 sea-to-air fluxes is a magnitude larger than the other mentioned sinks, we will neglect them in
 11 our estimates for CHBr_3 and CH_2Br_2 as they do not play a large role. Photolysis of CH_3I is
 12 very slow in comparison to halide substitution (Zika et al., 1984). The latter is suggested to be
 13 an important sink in the tropical ocean during low wind speeds (Jones and Carpenter, 2007),
 14 while large wind speeds favor sea-to-air fluxes as main sink (mean half-life of 8 days during
 15 MSM18/3). All three sink processes are included in our budget estimates using the rates
 16 published by Elliott and Rowland (1993). For CH_2I_2 , photolysis is the most significant sink in
 17 surface water (Jones and Carpenter, 2005). In our calculations, losses of CH_2I_2 due to
 18 photolysis were calculated according to Martino et al. (2006) with a photon flux calculated
 19 from the NASA COART model (Jin et al., 2006), a TChl *a* concentration of $0.4 \mu\text{g L}^{-1}$,
 20 absolute quantum yields from Martino et al. (2006), and absorption cross sections determined
 21 by Jones and Carpenter (2005).

22 **5.3.2 Mixed layer budget of halocarbons during MSM18/3**

23 In the following section, the results of the halocarbon budget calculations ~~for each station~~ are
 24 presented. The total mixed layer concentrations were calculated at every station considering a
 25 water column with a volume of $1 \times 1 \times z_{ML} \text{ m}^3$. Assuming that halocarbons are only produced
 26 below the mixed layer, the following relationship (equation 4) is valid for the steady state
 27 concentration C_{hal} , with F_{dia} and F_{adv} as the source terms from diapycnal fluxes and advection,
 28 while S_{as} (Figure 6) and S_{ch} represent the loss terms sea-to-air flux and chemical sinks as
 29 described in the previous section:

$$30 \quad C_{hal} = F_{dia} + F_{adv} - S_{as} - S_{ch} \quad (4)$$

31 S_{as} is the main sink term for CHBr_3 , CH_2Br_2 and CH_3I during MSM18/3 (Table 6). On the
 32 short time scales considered here, diapycnal fluxes of CH_3I , which can reduce the mixed layer
 33 by around 5 pmol per hour (Table 5), compete with the loss due to chloride substitution (S_{ch}).
 34 For CH_2I_2 , S_{ch} (photolysis) is about 10 times higher than S_{as} , and reduces the mixed layer

1 budget by 24 % after 1 h. In total, diapycnal fluxes (F_{dia}) into the mixed layer were not
 2 sufficient to account for the losses of all four compounds **from the mixed layer** (Table 6).
 3 The discrepancies **with respect to the total mixed layer** are 169 (CH_2Br_2), 255 (CH_3I), 269
 4 (CHBr_3) to 8382 (CH_2I_2) pmol h^{-1} , which are small compared to the total amount of
 5 halocarbons in the mixed layer (CHBr_3 – 0.17 %, CH_2Br_2 – 0.19 %, CH_3I – 0.34 %, CH_2I_2 –
 6 13.11 %). Possible reasons for the observed discrepancies are evaluated in the following.
 7 Advection of the missing halocarbons, F_{adv} , likely does not play a large role for CH_2Br_2 , CH_3I
 8 and CH_2I_2 , since mean mixed layer concentrations of these compounds were rather
 9 homogeneous in the whole region. Thus, **only** for CHBr_3 , with more variable concentrations,
 10 advection may transport significant amounts from one location to another. In addition,
 11 halocarbon maxima were found within the mixed layer, which may either result from a mixed
 12 layer that is not well mixed or halocarbon production is faster than mixing in the mixed layer.
 13 According to the temperature and salinity profiles during the whole cruise (Figure 3), the
 14 mixed layer was very well mixed. Consequently, production in the mixed layer is the most
 15 likely process balancing the missing halocarbons (Table 6) as diapycnal fluxes and advection
 16 play minor roles. The maxima that occasionally evolve in the mixed layer suggest that
 17 production of halocarbons is rapid, but may vary with depth. The mixed layer production
 18 term, here called P_{ML} , has to be included in the budget calculation of equation 4:

$$19 \quad C_{hal} = F_{dia} + F_{adv} - S_{as} - S_{ch} + P_{ML} \quad (5)$$

20 The relative production of halocarbons in the mixed layer is likely largest for CH_2I_2 , because
 21 its largest discrepancy arises from its rapid photolysis (up to 24 % loss in 1 h) (Table 6). This
 22 is in agreement to earlier studies investigating macroalgal production, proposing larger release
 23 rates of CH_2I_2 than of CHBr_3 , CH_2Br_2 and CH_3I (Klick and Abrahamsson, 1992; Carpenter et
 24 al., 2000).

25 **5.3.3 Production rates of halocarbons**

26 From the budget calculations, described in the previous section, potential production rates P_{ML}
 27 for the mixed layer are determined for each station. The mean production rates show large
 28 standard deviations (Table 7), including the variability and uncertainties in the estimated
 29 production rates. Production rates are 34 ± 65 (CHBr_3), 10 ± 12 (CH_2Br_2), 21 ± 24 (CH_3I),
 30 and 384 ± 318 $\text{pmol m}^{-3} \text{h}^{-1}$ (CH_2I_2). These are the first estimated production rates of CHBr_3
 31 and CH_2Br_2 for tropical phytoplankton species. For comparison to other studies, the
 32 production rates from this study are converted to rates per $\mu\text{g TChl } a$ (reported in Tables 3
 33 and 4), which results in mean (\pm standard deviation) production rates of $2.5 \times 10^{-3} \pm 4.5 \times 10^{-3}$

1 (CHBr₃), $8.4 \times 10^{-4} \pm 1.0 \times 10^{-3}$ (CH₂Br₂), $2.2 \times 10^{-3} \pm 3.0 \times 10^{-3}$ (CH₃I) and $3.3 \times 10^{-2} \pm 3.3 \times$
2 10^{-2} pmol [$\mu\text{g TChl } a$]⁻¹ h⁻¹ (CH₂I₂).

3 **5.3.4 Comparison to previously reported rates – CHBr₃ and CH₂Br₂**

4 Tokarczyk and Moore (1994) and Hughes et al. (2013) determined production rates from
5 polar algae **in laboratory studies** ranging between 2×10^{-3} and 2.1×10^{-2} pmol [$\mu\text{g Chl } a$]⁻¹ h⁻¹
6 ¹ on average for CHBr₃, depending on the growth phase, which is in the range of our
7 calculated rates. Production rates for CH₂Br₂ of on average $2.1 - 4.2 \times 10^{-3}$ pmol [$\mu\text{g Chl } a$]⁻¹
8 h⁻¹ were much higher than the ones calculated in our study (Tokarczyk and Moore, 1994).
9 Karlsson et al. (2008) published production rates of $2.6 - 9.3 \times 10^{-2}$ pmol [$\mu\text{g Chl } a$]⁻¹ h⁻¹ for
10 CHBr₃ (depending on the time of day) and $5 \times 10^{-4} - 3.6 \times 10^{-3}$ pmol [$\mu\text{g Chl } a$]⁻¹ h⁻¹ for
11 CH₂Br₂ from an in situ study in the Baltic Sea during a cyanobacterial bloom. Liu et al.
12 (2011) calculated 417 (CHBr₃) and 258 pmol m⁻³ h⁻¹ (CH₂Br₂) for the subtropical and
13 temperate eastern US coast, which are tenfold higher than the production rates determined
14 from our study (Table 7). The differences between these studies and ours may have several
15 origins. **The Taking an average production rate** for the total mixed layer during MSM18/3
16 does not take a potential variable production with depth into account. Second, the different
17 production rates determined in the monocultural studies (Tokarczyk and Moore, 1994;
18 Hughes et al., 2013) show large variations between different types of microalgae. Third, the
19 indirect estimates during MSM18/3 are afflicted by the uncertainties in the individual budget
20 terms, which are also expressed in the large standard deviations.

21 **5.3.5 Comparison to previously reported rates – CH₃I and CH₂I₂**

22 Production rates of CH₃I determined from *Prochlorococcus* vary significantly from 5.8×10^{-4}
23 to 9.4×10^{-2} pmol [$\mu\text{g Chl } a$]⁻¹ h⁻¹ (Smythe-Wright et al., 2006; Brownell et al., 2010). Hughes
24 et al. (2011) suggested this variability to be caused by different cell states, e.g. healthier cells
25 producing less CH₃I. While Scarratt and Moore (1999) determined rates from $8.3 \times 10^{-3} - 5.0$
26 $\times 10^{-2}$ pmol [$\mu\text{g Chl } a$]⁻¹ h⁻¹ from a red microalgal species, Karlsson et al. (2008) reported a
27 rate of 1.0×10^{-2} pmol CH₃I [$\mu\text{g Chl } a$]⁻¹ h⁻¹ from a cyanobacterial bloom in the Baltic Sea,
28 which is at the higher end of the range mentioned here. Our estimates lie well within these
29 cited ranges **of phytoplankton production rates** and are thus a reasonable assumption for the
30 CH₃I production strength of tropical algae (see section 5.1.2).

31 In contrast to the other three halocarbons, very few studies have actually determined
32 production rates of CH₂I₂ from phytoplankton. CH₂I₂ was shown to be produced in
33 comparatively larger concentrations than other halocarbons, but generally from fewer species
34 (six polar and temperate *diatom* species were tested, of which only two produced CH₂I₂)
35 (Moore et al., 1996). Martino et al. (2006) assumed a theoretical production rate of 17,000

1 pmol m⁻³ h⁻¹ in the tropical equatorial Atlantic. These were calculated from previously
2 reported CH₂CII fluxes based on the assumption that CH₂CII is mainly formed during the
3 photolysis of CH₂I₂ and that CH₂I₂ is only produced in the TChl *a* maximum. This rate
4 appears very large in comparison to our estimate and in comparison to the production rates of
5 the other halocarbons. We showed evidence that CH₂I₂ is not only produced within the TChl *a*
6 maximum but in the whole mixed layer, thus, lower average production rates seem more
7 plausible. CH₂I₂ together with CH₂CII have been suggested to be equally important carriers of
8 organoiodine into the troposphere (Saiz-Lopez et al., 2012), hence it is important to determine
9 specific phytoplankton production rates of CH₂I₂ in future studies.

10 Our calculated production rates of CHBr₃, CH₂Br₂ and CH₃I lie well within the ranges of
11 several laboratory and field studies of mostly temperate and polar algae, suggesting
12 production from tropical algae to be similarly significant. CH₂I₂ was shown to be produced in
13 larger rates than the other three compounds, but very rapid photolysis leads to lower sea
14 surface concentrations of this compound. However, considering the large ranges in reported
15 production rates of CHBr₃, CH₂Br₂, CH₃I and the lack of studies concentrating on CH₂I₂,
16 more incubation experiments are severely needed to constrain in situ production rates of
17 tropical algae. This information is crucial to evaluate the significance and contribution of the
18 tropical ocean with respect to halogen transport into the troposphere, and finally into the
19 stratosphere. Understanding the fate of halocarbons within the water column is an important
20 task to estimate their distribution and emissions from the future ocean.

21

22 **6 Summary and conclusions**

23 Increased biological production during the Atlantic Cold Tongue (ACT) caused elevated
24 CHBr₃ and CH₂Br₂ concentrations **of up to 44.7 pmol L⁻¹ and up to 9.2 pmol L⁻¹** within the
25 equatorial surface water with comparable concentrations to other tropical upwelling systems.
26 Both compounds showed similar distributions and maxima in the region where the Equatorial
27 Undercurrent (EUC) influences the surface water between 2° and 3° S with cooler water and
28 elevated nutrients. *Chrysophytes*, the dominating phytoplankton group in the equatorial
29 surface water, were likely involved in the bromocarbon production. In contrast to their similar
30 surface water occurrence, CHBr₃ and CH₂Br₂ showed different distributions in the water
31 column. While CHBr₃ was mostly elevated in shallower layers in close proximity to the TChl
32 *a* maximum, CH₂Br₂ frequently showed maxima in deeper water likely caused by an
33 additional source.

1 In contrast to other tropical Atlantic regions, correlations of CH₃I with CHBr₃ and with
2 biological parameters indicate biogenic formation of CH₃I during the ACT. **Moderate CH₃I**
3 **concentrations of up to 12.8 pmol L⁻¹ were measured in the surface water.** CH₂I₂ surface
4 water and mixed layer concentrations were lowest due to its strong photolysis **with maximum**
5 **values of only 3.7 pmol L⁻¹.** CH₂I₂ maxima below the mixed layer, suggest similar formation
6 pathways to CH₂Br₂ **likely possibly** tied to heterotrophic activities below the layers of
7 maximum production.

8 Sea-to-air fluxes were the most important sink **for from** the mixed layer **budget** of CHBr₃,
9 CH₂Br₂ and CH₃I, while photolysis was the main sink for CH₂I₂. For the first time,
10 halocarbon turbulent fluxes from and into the mixed layer were calculated using
11 microstructure measurements and halocarbon concentration gradients in the water column.
12 The significance of these diapycnal fluxes as a source for mixed layer halocarbons, suggested
13 by halocarbon maxima below the mixed layer, was evaluated in comparison to sea-to-air
14 fluxes and other sinks. All sinks of halocarbons from the mixed layer were much larger than
15 the diapycnal supply into the mixed layer. Hence, halocarbon production **from both biogenic**
16 **and photochemical pathways** in the entire mixed layer is the most important factor
17 contributing to marine emissions of these compounds.

18 Production rates of halocarbons were estimated from 13 profiles for the tropical mixed layer.
19 **Calculated** production rates **varied between the stations** and were **on average**: 34 ± 65
20 pmol m⁻³ h⁻¹ for CHBr₃, 10 ± 12 pmol m⁻³ h⁻¹ for CH₂Br₂, 21 ± 24 pmol m⁻³ h⁻¹ for CH₃I and
21 384 ± 318 pmol m⁻³ h⁻¹ for CH₂I₂ **with large variability between the different stations.**
22 These are generally in the range of rates reported from both monocultural and in situ
23 incubation studies for CHBr₃, CH₂Br₂ and CH₃I, while CH₂I₂ seems to be emitted in larger
24 concentrations from phytoplankton.

25 Our results show the need to conduct more process-related studies in the field. The first
26 consideration of diapycnal mixing revealed that maximum concentrations in the vicinity of
27 the TChl *a* maximum are insignificant for the mixed layer budget. Investigating the exact
28 mechanisms of formation, degradation and transport of halocarbons in the water column
29 remains an important task toward understanding current and future emissions of these
30 compounds. Understanding the actual processes that contribute to their concentrations and
31 distribution within the water column is crucial to predict their emissions. We therefore
32 suggest further mono-cultural incubation studies to determine species-dependent production
33 and consumption rates **as well as more.** Temporally resolved in situ incubations in different
34 depths within the water column in combination with diapycnal flux measurements **will help**

1 **to explain the profile shapes.** Further halocarbon emission studies in the tropical ocean in
2 different seasons are crucial to evaluate their importance **for the stratospheric halogen**
3 **loading** in a global perspective.

4

5 **Acknowledgements**

6 We thank the chief scientist of the cruise MSM18/3 Arne Körtzinger, as well as the captain,
7 the crew and the scientific crew **of RV *Maria S. Merian*** for all of their help. The authors
8 acknowledge Sonja Wiegmann for pigment analysis, Bettina Taylor for CHEMTAX
9 calculations, and Martina Lohmann for nutrient measurements. We thank Björn Fiedler for
10 providing the fluorescence sensor data. We also appreciate the helpful input of Christa
11 Marandino. Additionally, the authors acknowledge NASA for providing satellite MODIS-
12 Aqua data **of June and July 2011**. This work was part of the German research project
13 SOPRAN II **and III** (grant no. FKZ 03F0611A **and 03F0662A**) funded by the
14 Bundesministerium für Bildung und Forschung (BMBF), and was also supported by the EU
15 project SHIVA (grant no. FP7-ENV-2007-1-226224) and by the HGF Innovative Network
16 Fund (PHYTOOPTICS project).

1

2 **Tables**

3 Table 1. Mean (minimum – maximum) values of physical parameters (sea surface temperature (SST), sea surface salinity (SSS), and wind
 4 speed), surface biomass proxies (TChl *a*-H: TChl *a* from HPLC measurements, TChl *a*-F: TChl *a* determined from the continuously
 5 measuring fluorescence sensor), and sea surface concentrations, as well as sea-to-air fluxes of the four halocarbons CHBr₃, CH₂Br₂, CH₃I, and
 6 CH₂I₂ during the cruise MSM18/3.

| Parameter | SST | SSS | Wind speed | Biomass proxies | | Halocarbons | | | | | | | |
|-------------|-------|------|----------------------|-----------------------|------------------|-------------------------|---|---------------------------------|---|-------------------------|---|--------------------------------|---|
| | | | | TChl <i>a</i> -H | TChl <i>a</i> -F | CHBr ₃ | | CH ₂ Br ₂ | | CH ₃ I | | CH ₂ I ₂ | |
| | | | | | | Con- centrations | Sea-to-air fluxes | Con- centrations | Sea-to-air fluxes | Con- centrations | Sea-to-air fluxes | Con- centrations | Sea-to-air fluxes |
| Unit | [° C] | | [m s ⁻¹] | [µg L ⁻¹] | | [pmol L ⁻¹] | [pmol h ⁻¹ m ⁻²] | [pmol L ⁻¹] | [pmol h ⁻¹ m ⁻²] | [pmol L ⁻¹] | [pmol h ⁻¹ m ⁻²] | [pmol L ⁻¹] | [pmol h ⁻¹ m ⁻²] |
| Mean | 24.4 | 35.7 | 6.1 | 0.51 | 0.44 | 12.9 | 644 | 3.7 | 187 | 5.5 | 425 | 1.1 | 82 |
| Min | 22.1 | 34.5 | 0.3 | 0.10 | 0.06 | 1.8 | -146 | 0.9 | -3 | 1.5 | 34 | 0.3 | 3 |
| Max | 29.0 | 36.3 | 11.1 | 0.99 | 1.20 | 44.7 | 4285 | 9.2 | 762 | 12.8 | 1300 | 3.7 | 382 |

7

1 Table 2. Spearman's rank correlation coefficients r_s of halocarbons with different physical parameters and phytoplankton species measured in
 2 surface water. Numbers printed in bold are regarded as significant with $p < 0.05$.

| | CHBr ₃ | CH ₂ Br ₂ | CH ₃ I | CH ₂ I ₂ | SST | Salinity | Global radiation | Latitude | Wind speed | Chlorophyll a + Div a | Chlorophytes | Chrysophytes | Dinoflagellates | Haptophytes |
|----------------------|-------------------|---------------------------------|-------------------|--------------------------------|--------------|--------------|------------------|--------------|--------------|-----------------------|--------------|--------------|-----------------|-------------|
| Prochlorococcus (HL) | -0.70 | -0.57 | -0.21 | 0.27 | 0.44 | -0.39 | -0.20 | 0.49 | 0.26 | -0.01 | 0.34 | -0.28 | -0.14 | -0.33 |
| Haptophytes | 0.34 | 0.37 | 0.39 | -0.25 | -0.58 | 0.34 | 0.16 | -0.21 | -0.34 | 0.57 | -0.18 | 0.37 | 0.53 | |
| Dinoflagellates | 0.22 | 0.22 | 0.29 | -0.02 | -0.50 | 0.10 | -0.14 | -0.33 | -0.37 | 0.72 | 0.09 | 0.40 | | |
| Chrysophytes | 0.43 | 0.41 | 0.26 | 0.13 | -0.45 | 0.48 | -0.28 | -0.15 | -0.15 | 0.71 | 0.22 | | | |
| Chlorophytes | -0.29 | -0.26 | -0.15 | 0.32 | 0.13 | -0.15 | -0.26 | 0.25 | -0.05 | 0.11 | | | | |
| TChl <i>a</i> | 0.23 | 0.27 | 0.36 | 0.04 | -0.58 | 0.35 | -0.22 | -0.13 | -0.27 | | | | | |
| Wind speed | -0.18 | -0.16 | -0.22 | 0.20 | 0.56 | -0.06 | 0.12 | 0.04 | | | | | | |
| Latitude | -0.38 | -0.18 | 0.03 | 0.12 | 0.10 | -0.20 | -0.08 | | | | | | | |
| Global radiation | 0.05 | 0.04 | -0.09 | -0.25 | 0.19 | -0.09 | | | | | | | | |
| SSS | 0.48 | 0.41 | -0.09 | -0.04 | -0.42 | | | | | | | | | |

| | | | | |
|---------------------------------|--------------|--------------|--------------|-------------|
| SST | -0.46 | -0.46 | -0.42 | 0.33 |
| CH ₂ I ₂ | 0.07 | 0.09 | -0.04 | |
| CH ₃ I | 0.50 | 0.62 | | |
| CH ₂ Br ₂ | 0.90 | | | |

1

2 Table 3. Concentrations of CHBr₃, CH₂Br₂ and TChl *a* (from HPLC measurements) averaged over different depths at every CTD station (1 –
3 13), as well as the mixed layer depth. If a range is not given, only one measurement point exists. Bold numbers indicate the depth of
4 maximum concentrations at this station.

| | | 0 – 30 m | | 31 – 60 m | | 61 – 100 m | | | | |
|------------------------------|----|--|---------------------------------|-------------------------------------|--|----------------------------------|-------------------------------------|--|---------------------------------|-----|
| <i>z_{ML}</i> [m] | | Concentrations [pmol L ⁻¹] | | TChl <i>a</i> [μg L ⁻¹] | Concentrations [pmol L ⁻¹] | | TChl <i>a</i> [μg L ⁻¹] | Concentrations [pmol L ⁻¹] | | |
| | | CHBr ₃ | CH ₂ Br ₂ | | CHBr ₃ | CH ₂ Br ₂ | | CHBr ₃ | CH ₂ Br ₂ | |
| 1 | 34 | 5.4 (3.2 - 6.5) | 1.7 (1.3 - 2.1) | 0.60 (0.52 - 0.69) | 5.8 (3.7 - 7.9) | 3.0 (1.8 - 4.2) | 0.59 (0.53 - 0.65) | 2.1 | 1.1 | --- |

| | | | | | | | | | | |
|-----------|-----|----------------------|---------------------|---------------|---------------------|--------------------|---------------|-------------|--------------------|---------------|
| 2 | 16 | 30.2 | 6.5 | 0.92 | 9.0 | 5.2 | 0.86 | 2.4 | 1.8 | 0.20 |
| | | (25.4 - 35.0) | (6.4 - 6.6) | (0.76 - 1.07) | (7.6 - 10.3) | (5.1 - 5.4) | (0.74 - 0.97) | (1.2 - 4.6) | (0.8 - 3.6) | (0.10 - 0.30) |
| 3 | 37 | 6.8 | 3.9 | 0.80 | 3.0 | 2.4 | 0.65 | 2.3 | 2.3 | 0.18 |
| | | (6.2 - 7.4) | (3.6 - 4.2) | (0.75 - 0.86) | (2.6 - 3.2) | (2.4 - 2.5) | (0.51 - 0.80) | (2.2 - 2.5) | (2.3 - 2.3) | |
| 4 | 14 | 12.5 | 7.2 | 0.56 | 5.9 | 3.1 | 0.80 | 2.6 | 2.5 | 0.19 |
| | | (5.8 - 19.2) | (3.8 - 10.6) | (0.26 - 0.86) | (4.8 - 6.9) | (3.0 - 3.2) | (0.79 - 0.81) | (2.0 - 3.2) | (1.8 - 3.2) | (0.13 - 0.26) |
| 5 | 49 | 14.0 | 4.2 | 0.34 | | | | 7.6 | 7.4 | 0.39 |
| | | (13.6 - 14.4) | (4.0 - 4.3) | (0.28 - 0.39) | 11.7 | 4.8 | 0.58 | (6.6 - 8.5) | (6.1 - 8.6) | (0.24 - 0.53) |
| 6 | 12 | 13.4 | 5.0 | | 5.4 | 4.8 | 0.30 | 4.9 | 4.6 | 0.10 |
| | | (12.5 - 14.3) | (3.8 - 6.3) | 0.99 | (5.1 - 5.7) | (4.7 - 4.8) | (0.17 - 0.43) | (4.7 - 5.1) | (4.6 - 4.7) | (0.04 - 0.17) |
| 7 | --- | 11.2 | 4.6 | 0.71 | 3.7 | 3.4 | 0.46 | 3.1 | 3.0 | 0.11 |
| | | (8.8 - 13.7) | (3.5 - 4.6) | (0.65 - 0.76) | (2.5 - 4.9) | (2.5 - 4.2) | (0.44 - 0.48) | (2.9 - 3.4) | (2.9 - 3.1) | (0.06 - 0.17) |
| 8 | 45 | 5.0 | 1.0 | 0.34 | 7.0 | 2.5 | 0.51 | | | |
| | | (4.7 - 5.3) | (0.6 - 1.4) | (0.31 - 0.38) | (5.7 - 8.3) | (1.9 - 3.2) | (0.47 - 0.58) | 1.1 | 1.5 | 0.51 |
| 9 | 21 | 3.6 | 1.8 | 0.75 | 8.9 | 4.2 | 0.77 | 5.4 | 3.2 | 0.24 |
| | | (2.7 - 4.5) | (1.6 - 2.0) | (0.64 - 0.85) | (7.4 - 10.3) | (3.9 - 4.6) | (0.68 - 0.85) | (4.5 - 6.3) | (2.6 - 3.7) | (0.17 - 0.32) |
| 10 | 10 | 5.2 | 2.6 | 0.50 | 8.9 | 3.8 | 0.62 | 3.5 | 2.5 | 0.47 |
| | | (4.9 - 5.5) | (2.3 - 2.8) | (0.41 - 0.59) | (8.3 - 9.5) | (3.7 - 4.0) | (0.51 - 0.73) | (3.1 - 3.9) | (2.4 - 2.6) | (0.32 - 0.62) |

| | | | | | | | | | | |
|-----------|----|----------------------|--------------------|---------------|--------------|-------------|---------------|-------------|--------------------|------|
| 11 | 24 | 6.0 | 2.5 | 0.46 | 13.1 | 4.3 | 0.82 | 4.0 | 4.0 | 0.23 |
| | | (4.1 - 7.9) | (1.8 - 3.3) | (0.42 - 0.49) | | | | | | |
| 12 | 35 | 18.1 | 5.8 | 0.77 | 11.6 | 6.3 | 0.70 | 5.3 | 5.5 | 0.25 |
| | | (16.4 - 19.8) | (5.6 - 6.1) | (0.76 - 0.79) | (9.1 - 14.1) | (5.4 - 7.1) | (0.68 - 0.72) | (4.7 - 6.0) | (5.3 - 5.8) | |
| 13 | 41 | 11.6 | 3.5 | 0.55 | 8.9 | 4.6 | 0.16 | 5.9 | 5.2 | 0.12 |
| | | (6.9 - 16.4) | (2.5 - 4.4) | (0.51 - 0.58) | (8.3 - 9.5) | (3.0 - 5.6) | (0 - 0.48) | (3.3 - 7.6) | (4.1 - 5.7) | |

1

2 Table 4. Concentrations of CH₃I, CH₂I₂ and the sum of TChl *a* averaged over different depths at every CTD station (1 – 13), as well as the
3 mixed layer depth. If a range is not given, only one measurement point exists. Bold numbers indicate the depth of maximum concentrations at
4 this station.

| | | 0 – 30 m | | 30 – 60 m | | 60 – 100 m | | | | |
|------------------------------|----|---|--------------------------------|-------------------------------------|---|--------------------------------|-------------------------------------|---|--------------------------------|--|
| <i>z_{ML}</i> [m] | | Concentrations [pmol L ⁻¹] | | TChl <i>a</i> [μg L ⁻¹] | Concentrations [pmol L ⁻¹] | | TChl <i>a</i> [μg L ⁻¹] | Concentrations [pmol L ⁻¹] | | TChl <i>a</i> [μg L ⁻¹] |
| | | CH ₃ I | CH ₂ I ₂ | | CH ₃ I | CH ₂ I ₂ | | CH ₃ I | CH ₂ I ₂ | |
| 1 | 34 | 2.7 | 4.5 | 0.60 | 2.5 | 9.9 | 0.59 | 0.2 | 1.7 | --- |
| | | (2.1 - 3.4) | (1.2 - 6.8) | (0.52 - 0.69) | (1.8 - 3.2) | (3.9 - 16.0) | (0.53 - 0.65) | | | |

| | | | | | | | | | | |
|-----------|-----|---------------------|---------------------|---------------|--------------------|----------------------|---------------|-------------|---------------------|---------------|
| 2 | 16 | 2.8 | 4.8 | 0.92 | 3.1 | 12.2 | 0.86 | 0.6 | 2.0 | 0.20 |
| | | (0.4 - 5.2) | (1.7 - 8.0) | (0.76 - 1.07) | (2.7 - 3.6) | (11.5 - 12.9) | (0.74 - 0.97) | (0.1 - 1.3) | (0.7 - 4.3) | (0.10 - 0.30) |
| 3 | 37 | 8.5 | 4.1 | 0.80 | 2.6 | 4.6 | 0.65 | 0.7 | 3.3 | 0.18 |
| | | (8.4 - 8.5) | (1.7 - 6.4) | (0.75 - 0.86) | (1.0 - 3.5) | (4.3 - 4.9) | (0.51 - 0.80) | (0.4 - 1.1) | (2.3 - 4.4) | |
| 4 | 14 | 6.1 | 7.0 | 0.56 | 4.6 | 2.3 | 0.80 | 0.8 | 1.0 | 0.19 |
| | | (5.5 - 6.6) | | (0.26 - 0.86) | (4.6 - 4.7) | (2.2 - 2.4) | (0.79 - 0.81) | (0.7 - 0.9) | (0.7 - 1.3) | (0.13 - 0.26) |
| 5 | 49 | 5.4 | 0.6 | 0.34 | 4.5 | 4.9 | 0.58 | 2.4 | 10.5 | 0.39 |
| | | | (0.5 - 0.7) | (0.28 - 0.39) | | | | (1.9 - 3.0) | (7.1 - 13.8) | (0.24 - 0.53) |
| 6 | 12 | 10.4 | 6.9 | 0.99 | 1.6 | 4.0 | 0.30 | 1.4 | 2.4 | 0.10 |
| | | (8.0 - 12.8) | (1.8 - 12.0) | | (1.5 - 1.7) | (3.1 - 4.8) | (0.17 - 0.43) | (1.0 - 1.7) | (1.7 - 3.1) | (0.04 - 0.17) |
| 7 | --- | 4.1 | 2.3 | 0.71 | 1.3 | 4.7 | 0.46 | 0.9 | 2.0 | 0.11 |
| | | (3.4 - 4.8) | (1.2 - 3.4) | (0.65 - 0.76) | (1.2 - 1.3) | (3.3 - 6.1) | (0.44 - 0.48) | (0.6 - 1.2) | (1.5 - 2.7) | (0.06 - 0.17) |
| 8 | 45 | 0.2 | 0.3 | 0.34 | 4.7 | 1.2 | 0.51 | 0.0 | 2.4 | 0.51 |
| | | (0.1 - 0.4) | (0.3 - 0.3) | (0.31 - 0.38) | (3.0 - 7.0) | (0.5 - 1.9) | (0.47 - 0.58) | | | |
| 9 | 21 | 4.4 | 1.3 | 0.75 | 5.3 | 6.2 | 0.77 | 1.3 | 2.9 | 0.24 |
| | | (4.1 - 4.8) | (1.2 - 1.5) | (0.64 - 0.85) | (3.4 - 7.3) | (4.5 - 8.0) | (0.68 - 0.85) | (1.3 - 1.3) | (2.3 - 3.6) | (0.17 - 0.32) |
| 10 | 10 | 4.5 | 0.5 | 0.50 | 4.9 | 1.3 | 0.62 | 0.8 | 3.4 | 0.47 |
| | | (3.6 - 5.5) | (0.4 - 0.6) | (0.41 - 0.59) | (4.2 - 5.7) | (0.9 - 1.7) | (0.51 - 0.73) | (0.7 - 0.9) | (2.6 - 4.1) | (0.32 - 0.62) |

| | | | | | | | | | | |
|-----------|----|----------------------------------|--------------------|-----------------------|--------------------|----------------------------------|-----------------------|--------------------|----------------------------------|-----------------------|
| 11 | 24 | 3.8 (2.9 - 4.6) | 0.4 | 0.46 (0.42 - 0.49) | 4.4 | 2.3 | 0.82 | 1.7 (1.0 - 2.3) | 1.7 (0.6 - 3.2) | 0.23 (0.04 - 0.44) |
| 12 | 35 | 7.0 (6.8 - 7.1) | 1.2 (0.3 - 2.2) | 0.77 (0.76 - 0.79) | 2.7 | 4.1 (3.8 - 4.3) | 0.70 (0.68 - 0.72) | 2.0 | 2.7 (1.6 - 3.8) | 0.25 |
| 13 | 41 | 5.1 (4.3 - 5.9) | 1.5 (0.8 - 2.1) | 0.55 (0.51 - 0.58) | 3.8 (2.0 - 5.6) | 5.9 (3.9 - 7.4) | 0.16 (0 - 0.48) | 1.0 (0.1 - 2.0) | 3.4 (1.0 - 4.8) | 0.12 (0 - 0.30) |

1

2 Table 5. Diapycnal and sea-to-air fluxes at every CTD station for the four halocarbons. Positive fluxes in bold provide the mixed layer with
3 the corresponding halocarbon, while negative fluxes indicate losses from the mixed layer.

| CTD station | CHBr ₃ | | CH ₂ Br ₂ | | CH ₃ I | | CH ₂ I ₂ | |
|-------------|---|--|---|--|---|--|---|--|
| | Diapycnal flux [pmol m ⁻² h ⁻¹] | Sea-to-air flux [pmol m ⁻² h ⁻¹] | Diapycnal flux [pmol m ⁻² h ⁻¹] | Sea-to-air flux [pmol m ⁻² h ⁻¹] | Diapycnal flux [pmol m ⁻² h ⁻¹] | Sea-to-air flux [pmol m ⁻² h ⁻¹] | Diapycnal flux [pmol m ⁻² h ⁻¹] | Sea-to-air flux [pmol m ⁻² h ⁻¹] |
| 1 | 14 | 14 | 8 | -27 | 5 | -119 | 39 | -64 |
| 2 | -125 | -3651 | -8 | -689 | -13 | -44 | 29 | -199 |

| | | | | | | | | |
|-----------|----------|-------|----------|------|----------|------|-----------|------|
| 3 | 0 | -184 | 1 | -195 | -6 | -703 | 7 | -129 |
| 4 | 8 | -241 | 4 | -265 | -1 | -671 | 3 | --- |
| 5 | -3 | -893 | 4 | -275 | -2 | --- | 9 | -45 |
| 6 | 5 | -590 | 7 | -185 | -13 | -988 | 27 | -121 |
| 7 | --- | --- | --- | --- | --- | --- | --- | --- |
| 8 | -2 | -110 | -0 | -25 | -1 | -4 | 0 | -22 |
| 9 | 3 | -57 | 1 | -64 | 1 | -337 | 3 | -88 |
| 10 | 2 | -45 | -2 | -83 | -6 | -300 | -1 | -30 |
| 11 | 4 | -248 | 1 | -136 | 1 | -316 | 0 | -24 |
| 12 | -4 | -1208 | -1 | -357 | -2 | -583 | -0 | -20 |
| 13 | 1 | -837 | 0 | -231 | -3 | -446 | -4 | -54 |

1 Table 6. Total mixed layer budget of each halocarbon, potential sinks and sources (box size $1 \times 1 \times z_{ML}$ m³). The upper four rows indicate
 2 cases where diapycnal fluxes act as sources, while the lower four rows summarize the budget for the cases where the diapycnal fluxes were
 3 sinks for the mixed layer budget. “Other sinks” is halogen substitution for CH₃I and photolysis in case of CH₂I₂. The negative numbers
 4 indicate sinks for the budget.

| | Compound | z_{ML} | Total ML budget | Air-sea fluxes (S_{as}) | Diapycnal fluxes (F_{dia}) | Other sinks (S_{ch}) | Total after 1 h | Difference |
|-----------------------------------|---------------------------------|----------|-----------------|-----------------------------|--------------------------------|--------------------------|-----------------|--------------|
| Unit | | [m] | [pmol] | [pmol h ⁻¹] | [pmol h ⁻¹] | [pmol h ⁻¹] | [pmol] | [pmol] |
| | CHBr ₃ | 24 | 157543 | -274 | 5 | | 157274 | -269 |
| Diapycnal fluxes as source | CH ₂ Br ₂ | 29 | 90058 | -172 | 3 | | 89889 | -169 |
| | CH ₃ I | 26 | 75263 | -257 | 2 | 0 | 75004 | -255 |
| | CH ₂ I ₂ | 28 | 63947 | -78 | 13 | -8317 | 55565 | -8382 |
| | CHBr ₃ | 36 | 417098 | -1186 | -30 | | 415882 | -1216 |
| Diapycnal fluxes as sink | CH ₂ Br ₂ | 27 | 99604 | -236 | -2 | | 99366 | -238 |
| | CH ₃ I | 29 | 137560 | -420 | -5 | 0 | 137135 | -425 |
| | CH ₂ I ₂ | 29 | 106587 | -35 | -2 | -4977 | 101573 | -5014 |
| | | | | | | | | |

1

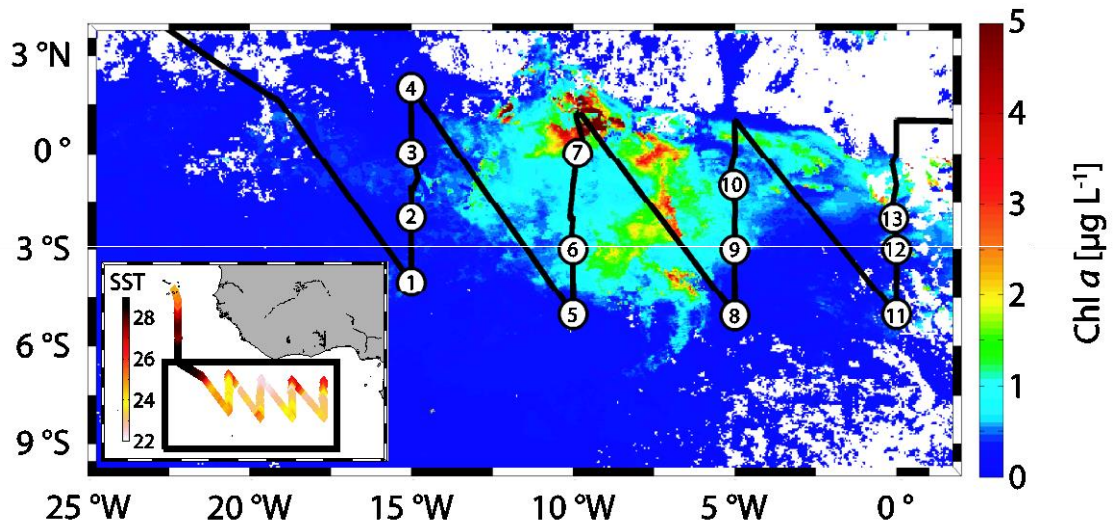
2 Table 7. Theoretical mean production rate of the four halocarbons in the equatorial mixed layer with the standard deviation.

| Compound | Production rate | Standard deviation | Production rate per TChl <i>a</i> |
|---------------------------------|---|---|---|
| | [pmol m ⁻³ h ⁻¹] | [pmol m ⁻³ h ⁻¹] | [pmol [μg TChl <i>a</i>] ⁻¹ h ⁻¹] |
| CHBr ₃ | 34 | 65 | 2.5 x 10 ⁻³ |
| CH ₂ Br ₂ | 10 | 12 | 8.5 x 10 ⁻⁴ |
| CH ₃ I | 21 | 24 | 2.2 x 10 ⁻³ |
| CH ₂ I ₂ | 384 | 318 | 3.3 x 10 ⁻² |

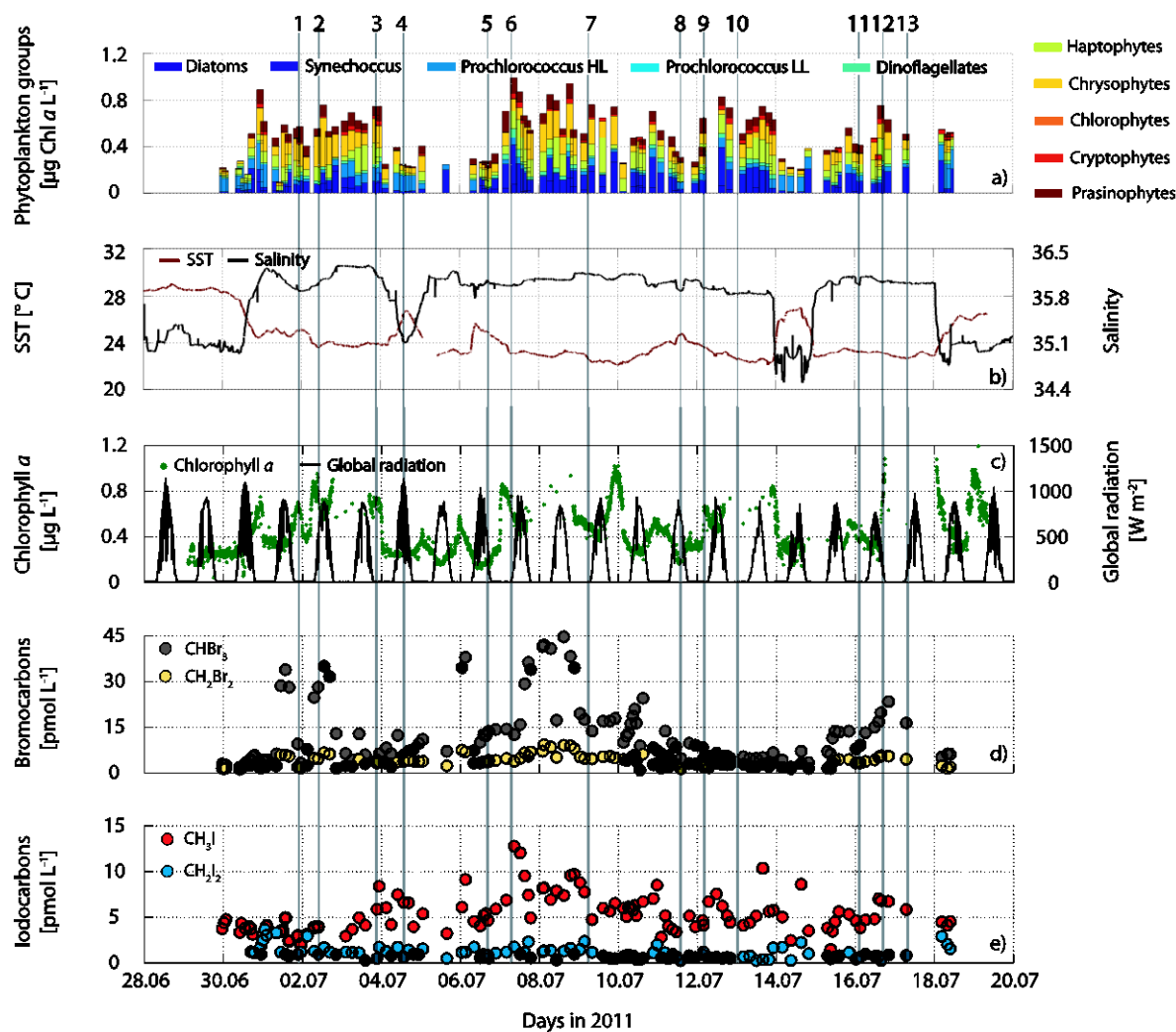
3

4

1 Figures

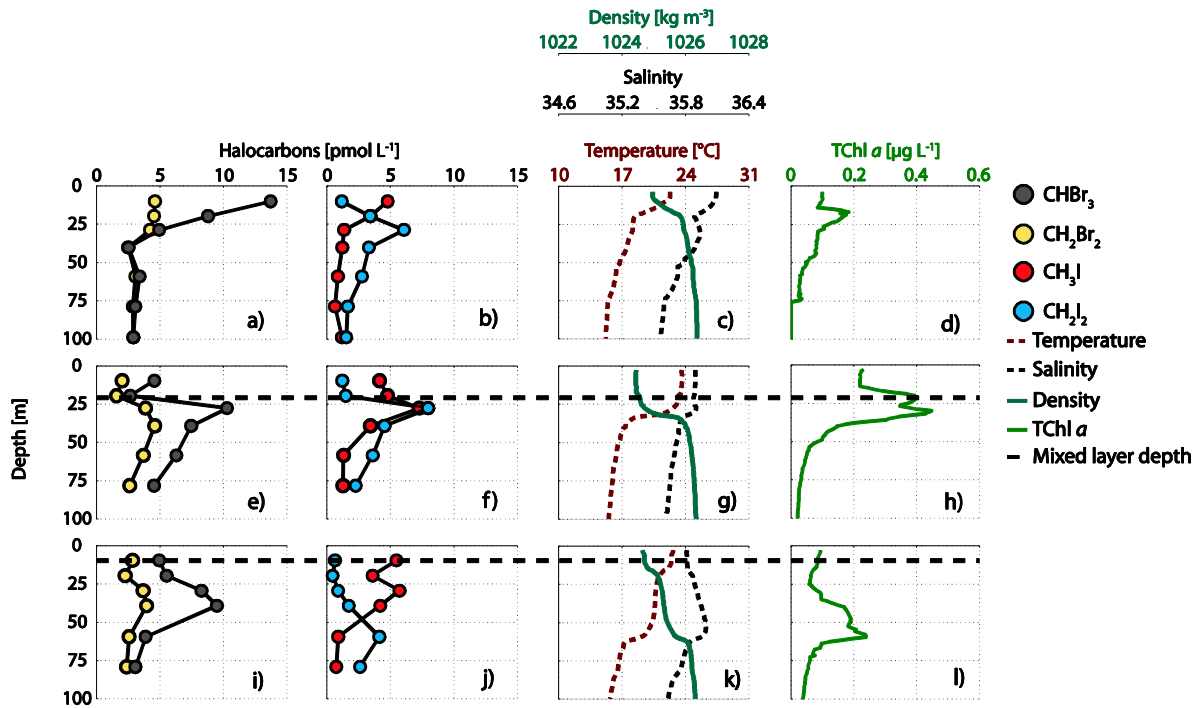


2
3 Figure 1. Cruise track with SST in °C (small box) and the section (large box) were
4 halocarbons were sampled in both the sea surface and during CTD stations (numbered
5 circles), plotted on monthly average Chl *a* for July 2011 derived from mapped level 3 MODIS
6 Aqua Data.



1
 2 Figure 2. a) Species composition (HL – high light, LL – low light), b) SST and salinity during
 3 the cruise, c) TChl a from underway fluorescence sensor measurements and global radiation,
 4 e) CHBr_3 and CH_2Br_2 in surface sea water, and e) CH_3I and CH_2I_2 surface sea water
 5 concentrations. The top numbers mark the CTD stations.

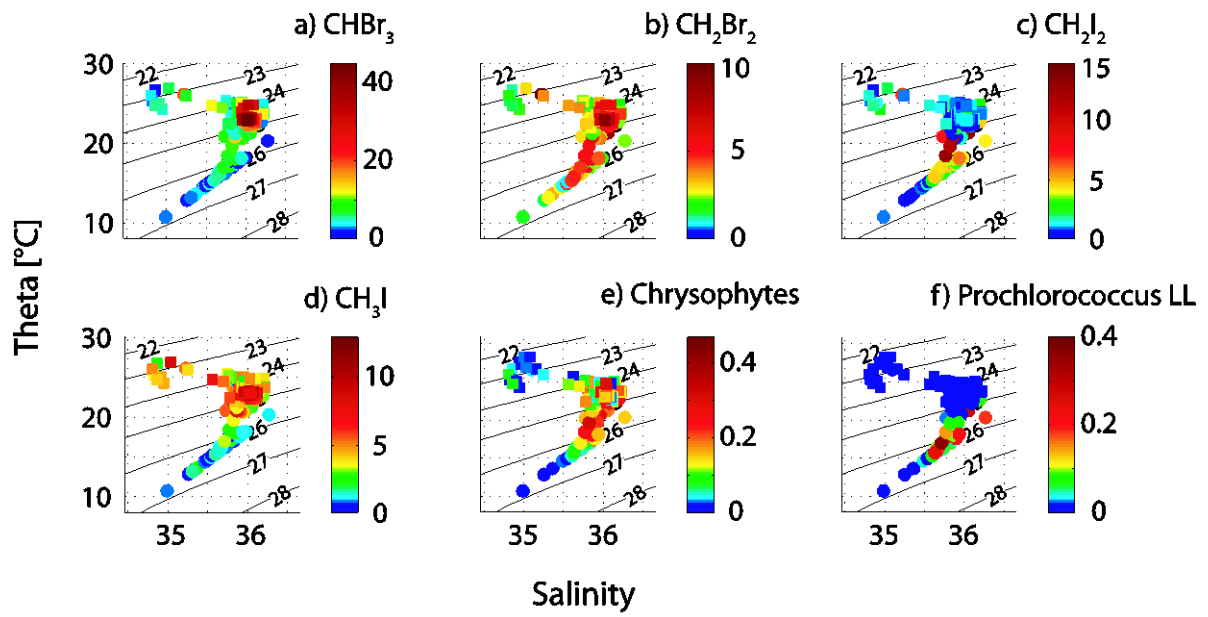
1



2

3 Figure 3. Selected CTD profiles (top – down: profiles 7, 9 and 10, see Figure 1 for the
4 location) of CHBr₃, CH₂Br₂, CH₃I, and CH₂I₂ in a – b), e – f), and i – j), along with
5 temperature, salinity, and density (c, g and k), as well as TChl *a* in d), h), and l), and the
6 mixed layer depth as black dashed line at the same stations.

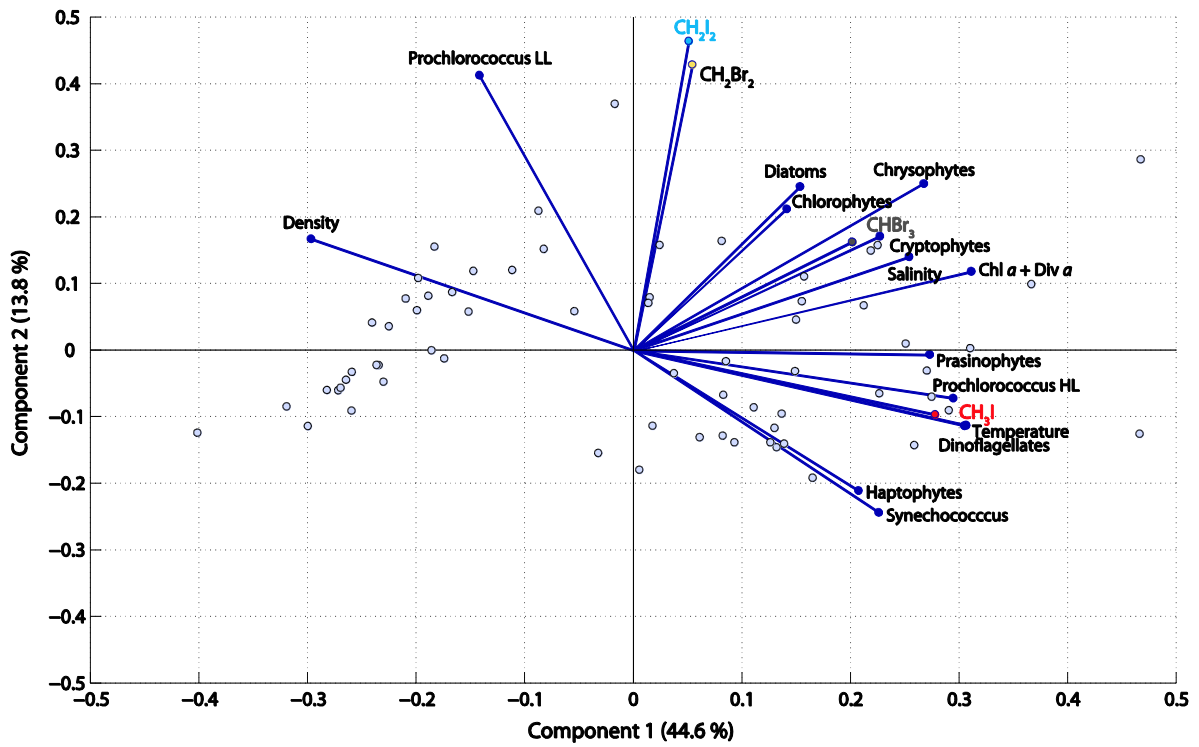
7



1

2 Figure 4. a – d) Temperature-Salinity (T-S) plots for halocarbons (in pmol L^{-1}) and e – f)
 3 phytoplankton species (in $\mu\text{g Chl } a \text{ L}^{-1}$). Square markers indicate surface values of
 4 halocarbons from underway measurements, circles are depth measurements from CTD
 5 profile, and the lines indicate the potential density – 1000.

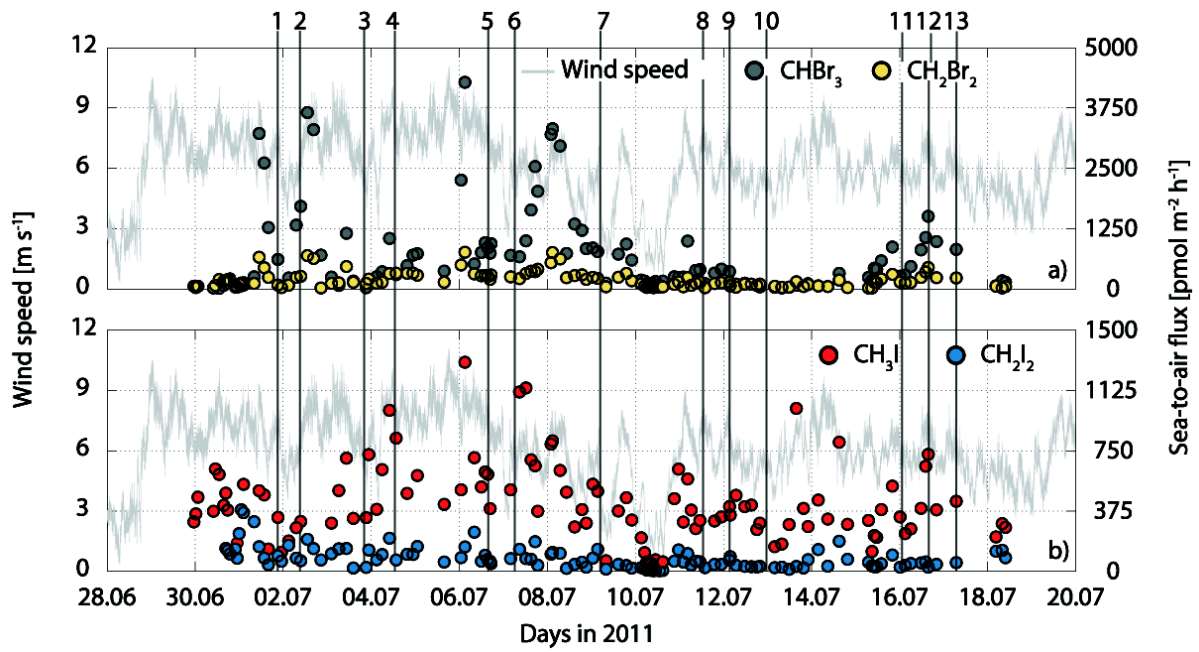
6



1

2 Figure 5. Principal component analysis (PCA) of halocarbon and phytoplankton species
 3 composition data, as well as temperature, salinity, and density for the 13 CTD stations during
 4 MSM18/3.

5



1
2
3
4
5

Figure 6. Wind speed during the cruise and sea-to-air fluxes calculated with sea surface water concentrations and mean atmospheric halocarbon data a) CHBr_3 and CH_2Br_2 and b) CH_3I and CH_2I_2 . Numbers on the top indicate CTD stations.

References

Abrahamsson, K., Bertilsson, S., Chierici, M., Fransson, A., Froneman, P. W., Loren, A., and Pakhomov, E. A.: Variations of biochemical parameters along a transect in the southern ocean, with special emphasis on volatile halogenated organic compounds, *Deep-Sea Res. Part II-Top. Stud. Oceanogr.*, 51, 2745-2756, 10.1016/j.dsr2.2004.09.004, 2004a.

Abrahamsson, K., Lorén, A., Wulff, A., and Wangberg, S. A.: Air-sea exchange of halocarbons: The influence of diurnal and regional variations and distribution of pigments, *Deep-Sea Res. Part II-Top. Stud. Oceanogr.*, 51, 2789-2805, 10.1016/j.dsr2.2004.09.005, 2004b.

Amachi, S., Kamagata, Y., Kanagawa, T., and Muramatsu, Y.: Bacteria mediate methylation of iodine in marine and terrestrial environments, *Applied and Environmental Microbiology*, 67, 2718-2722, 10.1128/aem.67.6.2718-2722.2001, 2001.

Amachi, S., Muramatsu, Y., Akiyama, Y., Miyazaki, K., Yoshiki, S., Hanada, S., Kamagata, Y., Ban-nai, T., Shinoyama, H., and Fujii, T.: Isolation of iodide-oxidizing bacteria from iodide-rich natural gas brines and seawaters, *Microb. Ecol.*, 49, 547-557, 10.1007/s00248-004-0056-0, 2005.

Amachi, S.: Microbial contribution to global iodine cycling: Volatilization, accumulation, reduction, oxidation, and sorption of iodine, *Microbes Environ.*, 23, 269-276, 10.1264/jsme2.ME08548, 2008.

Aschmann, J., Sinnhuber, B. M., Chipperfield, M. P., and Hossaini, R.: Impact of deep convection and dehydration on bromine loading in the upper troposphere and lower stratosphere, *Atmos. Chem. Phys.*, 11, 2671-2687, 10.5194/acp-11-2671-2011, 2011.

Barlow, R. G., Cummings, D. G., and Gibb, S. W.: Improved resolution of mono- and divinyl chlorophylls a and b and zeaxanthin and lutein in phytoplankton extracts using reverse phase c-8 hplc, *Marine Ecology Progress Series*, 161, 303-307, 10.3354/meps161303, 1997.

Bracher A., Taylor B.B., Taylor M., Dinter T., Röttgers R., Steinmetz F. (2015) Using empirical orthogonal functions derived from remote sensing reflectance for the prediction of concentrations of phytoplankton pigments. *Ocean Science* 11: 139-158.

Brownell, D. K., Moore, R. M., and Cullen, J. J.: Production of methyl halides by prochlorococcus and synechococcus, *Glob. Biogeochem. Cycles*, 24, 10.1029/2009gb003671, 2010.

Carpenter, L. J. and Liss, P. S.: On temperate sources of bromoform and other reactive organic bromine gases, *J. Geophys. Res.-Atmos.*, 105, 20539-20547, 10.1029/2000JD900242.

Carpenter, L. J., Malin, G., Liss, P. S., and Kupper, F. C.: Novel biogenic iodine-containing trihalomethanes and other short-lived halocarbons in the coastal east atlantic, *Glob. Biogeochem. Cycles*, 14, 1191-1204, 10.1029/2000GB001257, 2000.

Carpenter, L. J., Wevill, D. J., Palmer, C. J., and Michels, J.: Depth profiles of volatile iodine and bromine-containing halocarbons in coastal antarctic waters, *Mar. Chem.*, 103, 227-236, 10.1016/j.marchem.2006.08.003, 2007.

Carpenter, L. J., Jones, C. E., Dunk, R. M., Hornsby, K. E., and Woeltjen, J.: Air-sea fluxes of biogenic bromine from the tropical and north atlantic ocean, *Atmos. Chem. Phys.*, 9, 1805-1816, 10.5194/acp-9-1805-2009, 2009.

Claustre, H., and Marty, J. C.: Specific phytoplankton biomasses and their relation to primary production in the tropical north-atlantic, *Deep-Sea Res. Part I-Oceanogr. Res. Pap.*, 42, 1475-1493, 10.1016/0967-0637(95)00053-9, 1995.

Elliott, S., and Rowland, F. S.: Nucleophilic substitution rates and solubilities for methyl halides in seawater, *Geophys. Res. Lett.*, 20, 1043-1046, 10.1029/93gl01081, 1993.

Elliott, S., and Rowland, F. S.: Methyl halide hydrolysis rates in natural waters, *J. Atmos. Chem.*, 20, 229-236, 10.1007/bf00694495, 1995.

Fujiki, T., Matsumoto, K., Watanabe, S., Hosaka, T., and Saino, T.: Phytoplankton productivity in the western subarctic gyre of the north pacific in early summer 2006, *J. Oceanogr.*, 67, 295-303, 10.1007/s10872-011-0028-1, 2011.

Fuse, H., Inoue, H., Murakami, K., Takimura, O., and Yamaoka, Y.: Production of free and organic iodine by *roseovarius* spp, *FEMS Microbiology Letters*, 229, 189-194, 10.1016/s0378-1097(03)00839-5, 2003.

Geen, C. E.: Selected marine sources and sinks of bromoform and other low molecular weight organobromines, PhD, Dalhousie University, Halifax, Halifax, Nova Scotia, 1992.

Goodwin, K. D., Schaefer, J. K., and Oremland, R. S.: Bacterial oxidation of dibromomethane and methyl bromide in natural waters and enrichment cultures, *Applied and Environmental Microbiology*, 64, 4629-4636, 1998.

Grodsky, S. A., Carton, J. A., and McClain, C. R.: Variability of upwelling and chlorophyll in the equatorial atlantic, *Geophys. Res. Lett.*, 35, L03610, 10.1029/2007gl032466, 2008.

Happell, J. D., and Wallace, D. W. R.: Methyl iodide in the greenland/norwegian seas and the tropical atlantic ocean: Evidence for photochemical production, *Geophys. Res. Lett.*, 23, 2105-2108, 10.1029/96gl01764, 1996.

Hense, I., and Quack, B.: Modelling the vertical distribution of bromoform in the upper water column of the tropical atlantic ocean, *Biogeosciences*, 6, 535-544, 10.5194/bg-6-535-2009, 2009.

Hepach, H., Quack, B., Ziska, F., Fuhlbrügge, S., Atlas, E. L., Krüger, K., Peeken, I., and Wallace, D. W. R.: Drivers of diel and regional variations of halocarbon emissions from the tropical north east atlantic, *Atmos. Chem. Phys.*, 14, 1255-1275, 10.5194/acp-14-1255-2014, 2014.

Hopkins, F. E., Kimmance, S. A., Stephens, J. A., Bellerby, R. G. J., Brussaard, C. P. D., Czerny, J., Schulz, K. G., and Archer, S. D.: Response of halocarbons to ocean acidification in the arctic, *Biogeosciences*, 10, 2331-2345, 10.5194/bg-10-2331-2013, 2013.

Hossaini, R., Chipperfield, M. P., Monge-Sanz, B. M., Richards, N. A. D., Atlas, E., and Blake, D. R.: Bromoform and dibromomethane in the tropics: A 3-d model study of chemistry and transport, *Atmos. Chem. Phys.*, 10, 719-735, 10.5194/acp-10-719-2010, 2010.

Hossaini, R., Chipperfield, M. P., Feng, W., Breider, T. J., Atlas, E., Montzka, S. A., Miller, B. R., Moore, F., and Elkins, J.: The contribution of natural and anthropogenic very short-lived species to stratospheric bromine, *Atmos. Chem. Phys.*, 12, 371-380, 10.5194/acp-12-371-2012, 2012.

Hughes, C., Chuck, A. L., Rossetti, H., Mann, P. J., Turner, S. M., Clarke, A., Chance, R., and Liss, P. S.: Seasonal cycle of seawater bromoform and dibromomethane concentrations in a coastal bay on the western antarctic peninsula, *Glob. Biogeochem. Cycles*, 23, Gb2024, 10.1029/2008gb003268, 2009.

- Hughes, C., Franklin, D. J., and Malin, G.: Iodomethane production by two important marine cyanobacteria: *Prochlorococcus marinus* (ccmp 2389) and *synechococcus* sp (ccmp 2370), *Mar. Chem.*, 125, 19-25, 10.1016/j.marchem.2011.01.007, 2011.
- Hughes, C., Johnson, M., Utting, R., Turner, S., Malin, G., Clarke, A., and Liss, P. S.: Microbial control of bromocarbon concentrations in coastal waters of the western antarctic peninsula, *Mar. Chem.*, 151, 35-46, 10.1016/j.marchem.2013.01.007, 2013.
- Hummels, R., Dengler, M., and Bourles, B.: Seasonal and regional variability of upper ocean diapycnal heat flux in the atlantic cold tongue, *Prog. Oceanogr.*, 111, 52-74, 10.1016/j.pocean.2012.11.001, 2013.
- Itoh, N., Tsujita, M., Ando, T., Hisatomi, G., and Higashi, T.: Formation and emission of monohalomethanes from marine algae, *Phytochemistry*, 45, 67-73, 10.1016/s0031-9422(96)00786-8, 1997.
- Jin, Z. H., Charlock, T. P., Rutledge, K., Stamnes, K., and Wang, Y. J.: Analytical solution of radiative transfer in the coupled atmosphere-ocean system with a rough surface, *Appl. Optics*, 45, 7443-7455, 10.1364/ao.45.007443, 2006.
- Johnson, Z. I., Zinser, E. R., Coe, A., McNulty, N. P., Woodward, E. M. S., and Chisholm, S. W.: Niche partitioning among *prochlorococcus* ecotypes along ocean-scale environmental gradients, *Science*, 311, 1737-1740, 10.1126/science.1118052, 2006.
- Jones, C. E., and Carpenter, L. J.: Solar photolysis of ch_2i_2 , ch_2ici , and ch_2ibr in water, saltwater, and seawater, *Environ. Sci. Technol.*, 39, 6130-6137, 10.1021/es050563g, 2005.
- Jones, C. E., and Carpenter, L. J.: Chemical destruction of $ch_3ic_2h_5i$, c_2h_5i , $1-c_3h_7i$, and $2-c_3h_7i$ in saltwater, *Geophys. Res. Lett.*, 34, L13804, 10.1029/2007gl029775, 2007.
- Jones, C. E., Hornsby, K. E., Sommariva, R., Dunk, R. M., Von Glasow, R., McFiggans, G., and Carpenter, L. J.: Quantifying the contribution of marine organic gases to atmospheric iodine, *Geophys. Res. Lett.*, 37, L18804, 10.1029/2010gl043990, 2010.
- Jouanno, J., Marin, F., du Penhoat, Y., Sheinbaum, J., and Molines, J. M.: Seasonal heat balance in the upper 100 m of the equatorial atlantic ocean, *J. Geophys. Res.-Oceans*, 116, 10.1029/2010jc006912, 2011.
- Kara, A. B., Rochford, P. A., and Hurlburt, H. E.: An optimal definition for ocean mixed layer depth, *J. Geophys. Res.-Oceans*, 105, 16803-16821, 10.1029/2000jc900072, 2000.
- Karlsson, A., Auer, N., Schulz-Bull, D., and Abrahamsson, K.: Cyanobacterial blooms in the baltic - a source of halocarbons, *Mar. Chem.*, 110, 129-139, 10.1016/j.marchem.2008.04.010, 2008.
- Kirkham, A. R., Jardillier, L. E., Tiganescu, A., Pearman, J., Zubkov, M. V., and Scanlan, D. J.: Basin-scale distribution patterns of photosynthetic picoeukaryotes along an atlantic meridional transect, *Environ. Microbiol.*, 13, 975-990, 10.1111/j.1462-2920.2010.02403.x, 2011.
- Klick, S., and Abrahamsson, K.: Biogenic volatile iodated hydrocarbons in the ocean, *J. Geophys. Res.-Oceans*, 97, 12683-12687, 10.1029/92jc00948, 1992.
- Kolber, Z., and Falkowski, P. G.: Use of active fluorescence to estimate phytoplankton photosynthesis in-situ, *Limnol. Oceanogr.*, 38, 1646-1665, 10.4319/lo.1993.38.8.1646, 1993.
- Kurihara, M. K., Kimura, M., Iwamoto, Y., Narita, Y., Ooki, A., Eum, Y. J., Tsuda, A., Suzuki, K., Tani, Y., Yokouchi, Y., Uematsu, M., and Hashimoto, S.: Distributions of short-lived iodocarbons and biogenic trace gases in the open ocean and atmosphere in the western north pacific, *Mar. Chem.*, 118, 156-170, 10.1016/j.marchem.2009.12.001, 2010.

Laternus, F.: Marine macroalgae in polar regions as natural sources for volatile organohalogens, *Environ. Sci. Pollut. Res.*, 8, 103-108, 10.1007/bf02987302, 2001.

Lin, C. Y., and Manley, S. L.: Bromoform production from seawater treated with bromoperoxidase, *Limnol. Oceanogr.*, 57, 1857-1866, 10.4319/lo.2012.57.06.1857, 2012.

Liu, Y. N., Yvon-Lewis, S. A., Hu, L., Salisbury, J. E., and O'Hern, J. E.: Chbr(3), ch(2)br(2), and chlbr(2) in u.S. Coastal waters during the gulf of mexico and east coast carbon cruise, *J. Geophys. Res.-Oceans*, 116, C10004, 10.1029/2010jc006729, 2011.

Liu, Y. N., Yvon-Lewis, S. A., Thornton, D. C. O., Campbell, L., and Bianchi, T. S.: Spatial distribution of brominated very short-lived substances in the eastern pacific, *J. Geophys. Res.-Oceans*, 118, 2318-2328, 10.1002/jgrc.20183, 2013a.

Liu, Y. N., Yvon-Lewis, S. A., Thornton, D. C. O., Butler, J. H., Bianchi, T. S., Cambell, L., Hu, L., and Smith, R. W.: Spatial and temporal distributions of bromoform and dibromomethane in the atlantic ocean and their relationship with photosynthetic biomass, *J. Geophys. Res.-Oceans*, 118, 3950-3965, 10.1002/jgrc.20299, 2013b.

Liu, Y. N., Thornton, D. C. O., Bianchi, T. S., Arnold, W. A., Shields, M. R., Chen, J., and Yvon-Lewis, S. A.: Dissolved organic matter composition drives the marine production of brominated very short-lived substances, *Environ. Sci. Technol.*, 49, 3366-3374, 10.1021/es505464k, 2015.

Mabey, W., and Mill, T.: Critical review of hydrolysis of organic compounds in water under environmental conditions, *J. Phys. Chem. Ref. Data*, 7, 383-415, 10.1063/1.555572, 1978.

Mackey, M. D., Mackey, D. J., Higgins, H. W., and Wright, S. W.: Chemtax - a program for estimating class abundances from chemical markers: Application to hplc measurements of phytoplankton, *Mar. Ecol.-Prog. Ser.*, 144, 265-283, 10.3354/meps144265, 1996.

Manley, S. L., and Dastoor, M. N.: Methyl-iodide (ch₃i) production by kelp and associated microbes, *Mar. Biol.*, 98, 477-482, 10.1007/BF00391538, 1988.

Manley, S. L., and de la Cuesta, J. L.: Methyl iodide production from marine phytoplankton cultures, *Limnol. Oceanogr.*, 42, 142-147, 10.4319/lo.1997.42.1.0142, 1997.

Martino, M., Liss, P. S., and Plane, J. M. C.: The photolysis of dihalomethanes in surface seawater, *Environ. Sci. Technol.*, 39, 7097-7101, 10.1021/es048718s, 2005.

Martino, M., Liss, P. S., and Plane, J. M. C.: Wavelength-dependence of the photolysis of diiodomethane in seawater, *Geophys. Res. Lett.*, 33, L06606, 10.1029/2005gl025424, 2006.

Martino, M., Mills, G. P., Woeltjen, J., and Liss, P. S.: A new source of volatile organoiodine compounds in surface seawater, *Geophys. Res. Lett.*, 36, L01609, 10.1029/2008gl036334, 2009.

Molinari, R. L.: Observations of eastward currents in the tropical south-atlantic ocean - 1978 - 1980, *J. Geophys. Res.-Oceans and Atmospheres*, 87, 9707-9714, 10.1029/JC087iC12p09707, 1982.

Moore, R. M., and Tokarczyk, R.: Volatile biogenic halocarbons in the northwest atlantic, *Glob. Biogeochem. Cycles*, 7, 195-210, 10.1029/92GB02653, 1993.

Moore, R. M., and Zafiriou, O. C.: Photochemical production of methyl-iodide in seawater, *J. Geophys. Res.-Atmos.*, 99, 16415-16420, 10.1029/94jd00786, 1994.

Moore, R. M., Geen, C. E., and Tait, V. K.: Determination of henry law constants for a suite of naturally-occurring halogenated methanes in seawater, *Chemosphere*, 30, 1183-1191, 10.1016/0045-6535(95)00009-w, 1995a.

- Moore, R. M., Tokarczyk, R., Tait, V. K., Poulin, M., and Geen, C. E.: Marine phytoplankton as a natural source of volatile organohalogenes, in: Naturally-produced organohalogenes, edited by: Grimvall, A., and deLeer, E. W. B., Kluwer Academic Publishers, Dordrecht, 283-294, 1995b.
- Moore, R. M., Webb, M., Tokarczyk, R., and Wever, R.: Bromoperoxidase and iodoperoxidase enzymes and production of halogenated methanes in marine diatom cultures, *J. Geophys. Res.-Oceans*, 101, 20899-20908, 10.1029/96jc01248, 1996.
- Moore, R. M., and Groszko, W.: Methyl iodide distribution in the ocean and fluxes to the atmosphere, *J. Geophys. Res.-Oceans*, 104, 11163-11171, 10.1029/1998jc900073, 1999.
- Nightingale, P. D., Malin, G., and Liss, P. S.: Production of chloroform and other low-molecular-weight halocarbons by some species of macroalgae, *Limnol. Oceanogr.*, 40, 680-689, 10.4319/l0.1995.40.4.0680, 1995.
- Nightingale, P. D., Malin, G., Law, C. S., Watson, A. J., Liss, P. S., Liddicoat, M. I., Boutin, J., and Upstill-Goddard, R. C.: In situ evaluation of air-sea gas exchange parameterizations using novel conservative and volatile tracers, *Glob. Biogeochem. Cycles*, 14, 373-387, 10.1029/1999gb900091, 2000.
- Orlikowska, A., and Schulz-Bull, D. E.: Seasonal variations of volatile organic compounds in the coastal baltic sea, *Environ. Chem.*, 6, 495-507, 10.1071/en09107, 2009.
- Osborn, T. R.: Estimates of the local rate of vertical diffusion from dissipation measurements, *J. Phys. Oceanogr.*, 10, 83-89, 10.1175/1520-0485(1980)010<0083:eotlro>2.0.co;2, 1980.
- Penkett, S. A., Jones, B. M. R., Rycroft, M. J., and Simmons, D. A.: An interhemispheric comparison of the concentrations of bromine compounds in the atmosphere, *Nature*, 318, 550-553, 10.1038/318550a0, 1985.
- Philander, S. G. H., and Pacanowski, R. C.: A model of the seasonal cycle in the tropical atlantic ocean, *J. Geophys. Res.-Oceans*, 91, 14192-14206, 10.1029/JC091iC12p14192, 1986.
- Quack, B., and Wallace, D. W. R.: Air-sea flux of bromoform: Controls, rates, and implications, *Glob. Biogeochem. Cycles*, 17, 1023, 10.1029/2002gb001890, 2003.
- Quack, B., Atlas, E., Petrick, G., Stroud, V., Schauffler, S., and Wallace, D. W. R.: Oceanic bromoform sources for the tropical atmosphere, *Geophys. Res. Lett.*, 31, L23s05, 10.1029/2004gl020597, 2004.
- Quack, B., Atlas, E., Petrick, G., and Wallace, D. W. R.: Bromoform and dibromomethane above the mauritanian upwelling: Atmospheric distributions and oceanic emissions, *J. Geophys. Res.-Atmos.*, 112, D09312, 10.1029/2006jd007614, 2007a.
- Quack, B., Peeken, I., Petrick, G., and Nachtigall, K.: Oceanic distribution and sources of bromoform and dibromomethane in the mauritanian upwelling, *J. Geophys. Res.-Oceans*, 112, C10006, 10.1029/2006jc003803, 2007b.
- Raimund, S., Quack, B., Bozec, Y., Vernet, M., Rossi, V., Garçon, V., Morel, Y., and Morin, P.: Sources of short-lived bromocarbons in the iberian upwelling system, *Biogeosciences*, 8, 1551-1564, 10.5194/bg-8-1551-2011, 2011.
- Richter, U.: Factors influencing methyl iodide production in the ocean and its flux to the atmosphere, PhD, Mathematisch-Naturwissenschaftliche Fakultät der Christian-Albrechts-Universität zu Kiel, Christian-Albrechts-Universität zu Kiel, Kiel, 117 pp., 2004.
- Richter, U., and Wallace, D. W. R.: Production of methyl iodide in the tropical atlantic ocean, *Geophys. Res. Lett.*, 31, L23s03, 10.1029/2004gl020779, 2004.

Round, F. E.: The chrysophyta - a reassessment, in: *Chrysophytes: Aspects and problems*, edited by: Kristiansen, J., and Andersen, R. A., Cambridge University Press, Cambridge, 1986.

Saiz-Lopez, A., Plane, J. M. C., Baker, A. R., Carpenter, L. J., von Glasow, R., Martin, J. C. G., McFiggans, G., and Saunders, R. W.: Atmospheric chemistry of iodine, *Chem. Rev.*, 112, 1773-1804, 10.1021/cr200029u, 2012.

Scarratt, M. G., and Moore, R. M.: Production of methyl bromide and methyl chloride in laboratory cultures of marine phytoplankton ii, *Mar. Chem.*, 59, 311-320, 10.1016/s0304-4203(97)00092-3, 1998.

Scarratt, M. G., and Moore, R. M.: Production of chlorinated hydrocarbons and methyl iodide by the red microalga porphyridium purpureum, *Limnol. Oceanogr.*, 44, 703-707, 10.4319/lo.1999.44.3.0703, 1999.

Schafstall, J., Dengler, M., Brandt, P., and Bange, H.: Tidal-induced mixing and diapycnal nutrient fluxes in the mauritanian upwelling region, *J. Geophys. Res.-Oceans*, 115, C10014, 10.1029/2009jc005940, 2010.

Schall, C., Heumann, K. G., and Kirst, G. O.: Biogenic volatile organoiodine and organobromine hydrocarbons in the atlantic ocean from 42 degrees n to 72 degrees s, *Fresenius J. Anal. Chem.*, 359, 298-305, 10.1007/s002160050577, 1997.

Schauffler, S. M., Atlas, E. L., Flocke, F., Lueb, R. A., Stroud, V., and Travnicek, W.: Measurements of bromine containing organic compounds at the tropical tropopause, *Geophys. Res. Lett.*, 25, 317-320, 10.1029/98GL00040, 1998.

Schlundt, M., Brandt, P., Dengler, M., Hummels, R., Fischer, T., Bumke, K., Krahmann, G., and Karstensen, J.: Mixed layer heat and salinity budgets during the onset of the 2011 Atlantic cold tongue, *J. Geophys. Res.-Oceans*, 119, 7882-7910, 10.1002/2014jc010021, 2014.

Smythe-Wright, D., Boswell, S. M., Breithaupt, P., Davidson, R. D., Dimmer, C. H., and Diaz, L. B. E.: Methyl iodide production in the ocean: Implications for climate change, *Glob. Biogeochem. Cycles*, 20, Gb3003, 10.1029/2005gb002642, 2006.

Smythe-Wright, D., Peckett, C., Boswell, S., and Harrison, R.: Controls on the production of organohalogens by phytoplankton: Effect of nitrate concentration and grazing, *J. Geophys. Res.-Biogeosci.*, 115, 10.1029/2009jg001036, 2010.

Solomon, S., Garcia, R. R., and Ravishankara, A. R.: On the role of iodine in ozone depletion, *J. Geophys. Res.-Atmos.*, 99, 20491-20499, 10.1029/94jd02028, 1994.

Stramma, L., and Schott, F.: The mean flow field of the tropical atlantic ocean, *Deep-Sea Res. Part II-Top. Stud. Oceanogr.*, 46, 279-303, 10.1016/s0967-0645(98)00109-x, 1999.

Taylor, B. B., Torrecilla, E., Bernhardt, A., Taylor, M. H., Peeken, I., Rottgers, R., Piera, J., and Bracher, A.: Bio-optical provinces in the eastern atlantic ocean and their biogeographical relevance, *Biogeosciences*, 8, 3609-3629, 10.5194/bg-8-3609-2011, 2011.

Tegtmeier, S., Kruger, K., Quack, B., Atlas, E. L., Pisso, I., Stohl, A., and Yang, X.: Emission and transport of bromocarbons: From the west pacific ocean into the stratosphere, *Atmos. Chem. Phys.*, 12, 10633-10648, 10.5194/acp-12-10633-2012, 2012.

Tegtmeier, S., Krüger, K., Quack, B., Atlas, E., Blake, D. R., Boenisch, H., Engel, A., Hepach, H., Hossaini, R., Navarro, M. A., Raimund, S., Sala, S., Shi, Q., and Ziska, F.: The contribution of oceanic methyl iodide to stratospheric iodine, *Atmos. Chem. Phys.*, 13, 11869-11886, 10.5194/acp-13-11869-2013, 2013.

- Tokarczyk, R., and Moore, R. M.: Production of volatile organohalogenes by phytoplankton cultures, *Geophys. Res. Lett.*, 21, 285-288, 10.1029/94GL00009, 1994.
- Tomczak, M., and Godfrey, J. S.: Regional oceanography: An introduction, in, 2 ed., Daya Publishing House, Delhi, 2005.
- Tsuchiya, M., Talley, L. D., and McCartney, M. S.: An eastern atlantic section from iceland southward across the equator, *Deep-Sea Res.*, 39, 1885-1917, 10.1016/0198-0149(92)90004-d, 1992.
- Veldhuis, M. J. W., and Kraay, G. W.: Phytoplankton in the subtropical atlantic ocean: Towards a better assessment of biomass and composition, *Deep-Sea Res. Part I-Oceanogr. Res. Pap.*, 51, 507-530, 10.1016/j.dsr.2003.12.002, 2004.
- Wang, L., Moore, R. M., and Cullen, J. J.: Methyl iodide in the nw atlantic: Spatial and seasonal variation, *J. Geophys. Res.-Oceans*, 114, C07007, 10.1029/2007jc004626, 2009.
- Weingartner, T. J., and Weisberg, R. H.: On the annual cycle of equatorial upwelling in the central atlantic-ocean, *J. Phys. Oceanogr.*, 21, 68-82, 10.1175/1520-0485(1991)021<0068:otacoe>2.0.co;2, 1991.
- Yamamoto, H., Yokouchi, Y., Otsuki, A., and Itoh, H.: Depth profiles of volatile halogenated hydrocarbons in seawater in the bay of bengal, *Chemosphere*, 45, 371-377, 10.1016/s0045-6535(00)00541-5, 2001.
- Zika, R. G., Gidel, L. T., and Davis, D. D.: A comparison of photolysis and substitution decomposition rates of methyl-iodide in the ocean, *Geophys. Res. Lett.*, 11, 353-356, 10.1029/GL011i004p00353, 1984.
- Ziska, F., Quack, B., Abrahamsson, K., Archer, S. D., Atlas, E., Bell, T., Butler, J. H., Carpenter, L. J., Jones, C. E., Harris, N. R. P., Hepach, H., Heumann, K. G., Hughes, C., Kuss, J., Krüger, K., Liss, P., Moore, R. M., Orlikowska, A., Raimund, S., Reeves, C. E., Reifenhäuser, W., Robinson, A. D., Schall, C., Tanhua, T., Tegtmeier, S., Turner, S., Wang, L., Wallace, D., Williams, J., Yamamoto, H., Yvon-Lewis, S., and Yokouchi, Y.: Global sea-to-air flux climatology for bromoform, dibromomethane and methyl iodide, *Atmos. Chem. Phys.*, 13, 8915-8934, 10.5194/acp-13-8915-2013, 2013.